Research Square

Preprints are preliminary reports that have not undergone peer review.
They should not be considered conclusive, used to inform clinical practice,
or referenced by the media as validated information.

Metaproteomic portrait of the gut microbiome in children with Down syndrome

Valeria Marzano

valeria.marzano@opbg.net

Bambino Gesù Children's Hospital, IRCCS, Rome, Italy

Ilaria Pirona

Genome Up SRL

Federica Rapisarda

Bambino Gesù Children's Hospital, IRCCS, Rome, Italy

Chiara Marangelo

Bambino Gesù Children's Hospital, IRCCS, Rome, Italy

Gabriele Macari

Genome Up SRL

Stefano Levi Mortera

Bambino Gesù Children's Hospital, IRCCS, Rome, Italy

Pamela Vernocchi

Bambino Gesù Children's Hospital, IRCCS, Rome, Italy

Emanuele Agolini

Bambino Gesù Children's Hospital, IRCCS, Rome, Italy

Bruno Dallapiccola

Bambino Gesù Children's Hospital, IRCCS, Rome, Italy

Antonio Novelli

Bambino Gesù Children's Hospital, IRCCS, Rome, Italy

Simone Gardini

Genome Up SRL

Alberto Villani

Bambino Gesù Children's Hospital, IRCCS, Rome, Italy

Diletta Valentini

Bambino Gesù Children's Hospital, IRCCS, Rome, Italy

Lorenza Putignani

Bambino Gesù Children's Hospital, IRCCS, Rome, Italy

Article

Keywords: Trisomy 21, Down syndrome, pediatric patients, gut microbiome, metaproteomics

Posted Date: September 1st, 2026

DOI: https://doi.org/10.21203/rs.3.rs-10623142/v1

License: This work is licensed under a Creative Commons Attribution 4.0 International License.
Read Full License

Additional Declarations: Competing interest reported. Pirona I., Macari G., and Gardini S. were employed by GenomeUp. All other authors declare no potential conflict of interest.

Metaproteomic portrait of the gut microbiome in children with Down syndrome

Marzano Valeria[1,†,*], Pirona Ilaria[2,†], Rapisarda Federica[1], Marangelo Chiara[1], Macari Gabriele[2], Levi Mortera Stefano[1,$], Vernocchi Pamela[1], Emanuele Agolini[3], Bruno Dallapiccola[4], Antonio Novelli[3], Gardini Simone[2,‡], Alberto Villani[5,‡], Valentini Diletta[6,‡], Putignani Lorenza[7,8,‡,*]

[1] Microbiome Unit, Management and Diagnostic Innovations & Clinical Pathways Research Area, Bambino Gesù Children's Hospital, IRCCS, Rome, Italy

[2] GenomeUp, Rome, Italy

[3] Laboratory of Medical Genetics, Translational Cytogenomics Research Unit, Bambino Gesù Children's Hospital, IRCCS, Rome, Italy

[4] Medical Genetics Unit, Academic Department of Pediatrics, Bambino Gesù Children's Hospital, IRCCS, Rome, Italy.

[5] General Pediatrics, Infectious Disease and ED II Level Unit, Bambino Gesù Children's Hospital, IRCCS, Rome, Italy

[6] General Pediatric Follow-Up Unit, Bambino Gesù Children's Hospital, IRCCS, Rome, Italy

[7] Unit of Microbiomics, Unit of Microbiology and Diagnostic Immunology, and Microbiome Unit, Management and Diagnostic Innovations & Clinical Pathways Research Area, Bambino Gesù Children's Hospital, IRCCS, Rome, Italy

[8] Department of Life Sciences, Health and Health Professions, Link Campus University, Rome, Italy

[†] These authors have contributed equally to this work and share first authorship

[$] Current affiliation: Chromatography and Mass Spectrometry Core Facility, Bambino Gesù Children's Hospital, IRCCS, Rome, Italy

[‡] These authors share last authorship

[*] Correspondence to: Valeria Marzano, valeria.marzano@opbg.net; Lorenza Putignani, lorenza.putignani@opbg.net

Abstract

Down syndrome (DS), or Trisomy 21, is a genetic condition caused by an extra copy of chromosome 21, and is associated with a broad spectrum of comorbidities, including autoimmune, behavioral and gastrointestinal disorders. Because metaproteomics captures the proteins the gut microbiota (GM) actually expresses, it can clarify how the GM tracks these clinical manifestations. Forty-eight children with DS were enrolled in the study and stratified by age and comorbidity such as autoimmune thyroid diseases (AITDs), immune-related conditions, and behavioral disorders. Fecal proteins were extracted by differential centrifugation, trypsin-digested and analyzed by data-dependent nanoliquid chromatography coupled with tandem mass spectrometry, followed by MetaLab-MAG and Unipept processing. This resulted in the identification of bacterial and human protein groups (PGs), along with their label-free quantification, functional annotation, and taxonomic assignment. The GM metaproteome was shaped by age, but not by sex. In both age groups ($6 \leq$ years < 13 and $13 \leq$ years ≤ 18), comorbidity was consistently associated with pathway down-regulation: sulfur metabolism in AITDs; glycolysis/gluconeogenesis, pyruvate metabolism, oxidative phosphorylation and butanoate metabolism in immune-related conditions; and sixteen shared amino-acid, nucleotide, sugar and glycan pathways in behavioral disorders. This functional contraction was carried by a recurring set of taxa, including the butyrogenic *Faecalibacterium prausnitzii*, *Blautia* and *Ruminococcus bromii*. Comorbidity in DS is accompanied by a hypofunctional, short-chain fatty acid-poor microbiota, while the fecal host proteome mirrors processes associated with T21, including matrix remodeling and interferon-skewed immunity. These findings may open new avenues for therapeutic interventions aimed at improving pathological outcomes in DS.

Keywords: Trisomy 21; Down syndrome; pediatric patients; gut microbiome; metaproteomics

1 Introduction

Down syndrome (DS) is a genetic disorder caused by an extra copy or significant portion of the human chromosome 21. Consequently, it is frequently referred to as Trisomy 21 (T21). This condition, the most common chromosomal abnormality in humans, leads to intellectual disability and other numerous developmental anomalies and comorbidities, including facial dysmorphology, congenital heart defects, and structural and functional gastrointestinal (GI) abnormalities, mainly due to alterations of the enteric nervous system [1–3]. Usually, the onset of DS occurs during prenatal development; however, some manifestations may not become apparent until adulthood. Individuals with DS have an increased risk of developing hypothyroidism, autoimmune diseases, obstructive sleep apnea, epilepsy, hearing and vision problems, hematological disorders, recurrent infections, anxiety disorders, and early-onset Alzheimer's disease (AD) [4–6]. In DS, GI disturbances are intricately linked to the gut microbiota (GM) via the gut-brain axis (GBA), a complex, bidirectional communication network. The microbiota plays an active role in regulating this axis through neural, immune, endocrine, and humoral pathways, influencing the production of critical signaling molecules, such as short-chain fatty acids (SCFAs) and neurotransmitters. Thus, a dysbiotic gut environment in DS may contribute to both the GI pathophysiology or emotional and cognitive impairments. Indeed, the impact of GM dysbiosis on early brain development, in conjunction with its correlations with neurodevelopmental disorders, both genetic and non-genetic, and the manner in which signals from the GM may influence neuroplasticity and brain development during childhood, are subjects of considerable interest [7]. This motivates therapeutic strategies aimed at modulating the microbiome through probiotics, prebiotics, and diet [8]. Based on the GBA framework in DS, emerging evidence is showing an interesting link between GM and various DS-related comorbidities. A recent study has provided preliminary evidence on GM alterations present in adults with DS who may have mild cognitive impairment, the latter resembling patterns also seen in sporadic AD [9]. This finding provides further evidence that GM dysbiosis may contribute to the pathogenesis of early AD in DS, possibly through inflammatory and gut-brain signaling pathways, potentially serving as a novel target for future therapeutic interventions. To date, very few studies have characterized GM ecology in DS subjects [10–12], strictly distinguishing DS patients from healthy subjects.

A study have reported that subjects with DS exhibit distinct alterations in the gut microbial composition, with increased *Prevotella*, *Escherichia* or *Shigella* distributions, altered Firmicutes/Bacteroidetes ratio, often paired with pro-inflammatory profiles and metabolomic alterations [11].

In a mouse model transplanted with DS-associated GM, behavioral changes similar to depression and motor impairment can be reproduced [11]. Previous studies on GM and DS correlations evidenced GM profile modulation both in adults [10] and children [12].

Regardless of the different targeted-metagenomics approaches used in these studies, the shared evidence underlined behavioral indices to be correlated with an increase in *Parasporobacterium* and *Sutterella* and a decrease in *Acidaminococcaceae*, respectively.

Moreover, certain species of *Blautia* were found to correlate with cognitive dysfunction [13]. Besides sequencing-based characterization of GM ecology, a metaproteomics approach may actually provide a link between taxonomic and functional profiles.

With this purpose, the herein study explored the GM metaproteome in pediatric subjects with DS using a high-throughput mass spectrometry approach. Gut metaproteome modulations were found to be age-dependent in these children, mirroring findings previously reported in neurotypical subjects. We explored whether the co-occurrence of behavioral or immune-mediated comorbidities influences the GM metaproteomic landscape at ages previously identified as key drivers of GM compositional changes in children [14, 15], providing new potential implications for long-term pediatric clinical management and novel therapeutic strategies.

2 Subjects and Methods

2.1. Subjects' cohort and sample collection

Forty-eight children with DS, aged 6 to 18 years, were enrolled at the General Pediatric Follow-Up Unit of the Bambino Gesù Children's Hospital (OPBG) and Research Institute of Rome, Italy, between July 11, 2022 and February 28, 2023. Patients were diagnosed by karyotype analysis for carrying complete or mosaic T21.

Demography and clinical data were extracted from medical records for providing patient's metadata, including severity of cognitive impairment and gastrointestinal symptoms. Subjects who had taken antibiotics, probiotics, fermented milks, or other functional foods within the two weeks prior to fecal sample collection were excluded from the study.

To study GM by a metaproteomic approach, stool samples were collected at annual check-ups and stored at -80°C at the Unit of Microbiome until their use for experimental activities.

2.2. Sample processing

Proteins from frozen stools were extracted and digested as described in Levi Mortera *et al*. [16]. In summary, material was gradually thawed, 300 mg were weighted, and then suspended in 6 ml of ice-cold phosphate buffer. The suspension was then vortexed and shaken until complete dissolution occurred. Subsequently, differential centrifugation was employed (initial low-speed centrifugation, followed by bacterial cell pelleting through highspeed centrifugation) to increase the pellet yield in bacterial cells [17].

Bacterial enriched-pellet was then treated by adding 300 µL of lysis buffer (4 % sodium dodecyl sulphate, 100 mM dithiothreitol in 50 mM Tris-HCl pH 8, with addition of Halt Protease and Phosphatase Inhibitor Cocktail [Thermo Fisher Scientific, Waltham, MA, USA]). Samples were heated at 95°C; sonicated applying 25% amplitude (32.5 W) for 3 cycle of 30 s (VCX 130, VibraCell Ultrasonic Liquid Processor, Sonics & Materials Inc, Newtown, CT, USA) and centrifuged. Finally, protein quantification was performed by 2-D Quant kit (Cytiva Europe GmbH, Buccinasco [MI], Italy).

Fifty µg of proteins were subjected to reduction of disulfide bonds, alkylation, and digestion with Sequencing Grade Modified Trypsin (Promega, Milan, Italy) at a ratio 1:50 (w:w) enzyme to sample for 16 h by filter-aided sample preparation (FASP) protocol [18].

Peptides were eluted from the Microcon-10kDa Centrifugal Filter Units (Merck Millipore, Billerica, MA, USA), speed-vac dried and resuspended in 2% acetonitrile (ACN), 0.1% trifluoracetic acid (TFA) and 97.9 % water. The total peptide content was determined by NanoDrop 2000 (Thermo Fisher Scientific), employing a standard curve of MassPrep *Escherichia coli* digestion (Waters, Milford, Massachusetts, USA).

2.3. Chromatographic separation and mass spectrometry

Peptides were analysed by a nano liquid chromatography – electrospray ionization - tandem mass spectrometry (nLC-ESI-MS/MS) platform comprising an Ultimate 3000 RSLC chromatographic system coupled to an Orbitrap Exploris 480 mass spectrometer (Thermo Fisher Scientific) through a nanoESI source (EASY-Spray NG).

Peptide separation was performed with an EASY-Spray PepMap RSLC C18 column (2 µm particle size, 100 Å pore size, 75 µm i.d. x 50 cm length, Thermo Fisher Scientific) hyphenated with a µ-precolumn C18 PepMap100 (5 µm particle size, 100 Å pore size, 300 µm i.d. x 5mm length, Thermo Fisher Scientific) to concentrate and desalt the samples. Two µg of peptides were loaded on the precolumn at 10 µL/min (2% ACN, 0.1% TFA in water) for 3 minutes. Reverse-phase chromatography was performed at a flow rate of 250 nL/min using a linear gradient from 5 to 25% of organic solvent (99.9 % ACN and 0.1% formic acid [FA]) in 147 min, total LC-run of 190 min, and temperature of 40°C. MS analysis was done with Orbitrap full MS scan from 350 to 1,500 *m/z* at a resolving power of 120 K and positive ionization mode (2,000 V and 280 °C temperature of the ion transfer tube), with 30% normalized AGC target and maximum injection time of 50 ms.

Data-dependent MS/MS scan of the most abundant 20 signals was performed setting the Orbitrap resolution at 15,000, after higher-energy C-trap dissociation (HCD) with normalized collision energy of 30% and normalized AGC target of 50%. Quadrupole isolation with a 1.6 m/z isolation window was used and the intensity threshold for MS/MS was set to 8,000 and dynamic exclusion was enabled for 30 seconds. For internal calibration, a lock mass of the polydimethylcyclosiloxane (445.12003 m/z) was used. Two technical replicates were acquired for each sample.

2.4 Bioinformatic and statistical analyses of metaproteomics data

The MetaLab-MAG desktop version 1.0.2 software [19] was utilized to analyze nanoLC-ESI-MS/MS data. The following settings were configured: carbamidomethylation of cysteine as a fixed modification, protein N-terminal acetylation and oxidation of methionine as variable modifications, and a maximum of two missed cleavages. The Unified Human Gastrointestinal Genome (UHGG) v2.0.1 [20, 21] and the host UniProtKB/Swiss-Prot database (*Homo sapiens*) protein database were interrogated. The Lowest Common Ancestor (LCA) algorithm, executed via the Unipept CLI (command-line interface) version 4.0.1, was employed to assign the taxonomic annotation to the peptides. The output files from MetaLab-MAG and Unipept were collapsed to create a final comprehensive matrix using R version 4.3.1 *ad hoc* scripts, as previously described [17]. Protein groups (PGs) that exhibited a number of detected razor peptides less than three and were not present in both technical replicates were filtered out. The mean Label-Free Quantitation (LFQ) intensity values of PGs from the two technical replicates were calculated and then expressed as base 10 log

units. Only PGs identified in at least 50% of the whole sample set were retained and missing values were imputed by the K-nearest neighbors' method using a neighborhood of √samples. The final matrix incorporated PGs' LFQ intensities abundances, their functional annotations (*e.g.*, Clusters of Orthologous Groups [COG] name and category; Kyoto Encyclopedia of Genes and Genomes [KEGG] pathways [22, 23]) and their taxonomic assignment at all possible levels based on LCA rank. Multivariate analyses including Bray-Curtis β-diversity and Principal Component Analysis (PCA) were performed in R v.4.4.1 with the packages Vegan 2.6 and Ecodist 2.3.1. To test association between covariates and β-diversity, permutational multivariate analysis of variance (PERMANOVA, 999 permutations) was employed. The Partial Least Squares-Discriminant Analysis (PLS-DA) analysis was performed also in the R version 4.4.1 environment using the PLS function of the mixOmics 6.28.0 package. PLSDA statistics were obtained by means of fivefold cross validation and 1,000 permutations.

To assess data normality, Shapiro test, implemented within the Phyton scipy v 1.10.1 library (Python version 3.11.10 environment), was employed. Also, the Mann-Whitney test, executed to identify differential individual PGs between two groups based on the PGs' LFQ intensity abundances, exploited the Phyton scipy v 1.10.1 library. The values were filtered through $\log_{10}$(fold change, FC) values ≥ 0.3 or ≤ -0.3, which represents the ratio of the mean intensity of one group PG to the mean intensity of the other group' PG, and p-value < 0.05.

Differentially expressed KEGG pathways were computed considering the mean abundance of PGs intensity with the same KEGG pathways for each sample in each sample groups, applying a Mann-Whitney test, and selecting terms with false discovery rate (FDR)-adjusted p-values (using Benjamini-Hochberg correction) of < 0.05 (statsmodels v.0.14.0). For result visualization, cluster analysis was performed. Hierarchically-clustered heatmaps were generated using the seaborn.clustermap function (Seaborn 0.13.2, Python version 3.11.10 environment), with clustering based on average linkage and Euclidean distance metrics.

The Protein Analysis Through Evolutionary Relationships (PANTHER) classification system (http://www.pantherdb.org) (version 19.0 Released 2024-06-20) [24] web application, and FunRich (version 3.1.3) [25] were employed to investigate the identified PGs of human origin. Human PGs localization and function annotation were retrieved and process enrichment analysis for human pathway were performed applying a Fisher's Exact test and FDR-adjusted p-values (Bonferroni correction) of < 0.05 (PANTHER Overrepresentation Test [Released 20240807]). Furthermore, comparative pathway analysis was performed on the LFQ values of the differentially expressed human PGs using ReactomeGSA (Reactome, version 94 released on September 17, 2025,

https://reactome.org/gsa/home) [26] with the following parameters: Camera analysis algorithm, interactors used, no disease pathways included, and no normalization function applied.

3 Results

3.1 The GM metaproteome of children with Down syndrome is influenced by age, but not by sex

Forty-eight subjects with DS, ranging in age from six to 18 years (mean age 11 ± 4 years), 34 males and 14 females, male sex frequency of 71%, were enrolled (**Supplementary file 1**). Subjects were stratified also into two age groups: age group 1 (6 ≤ years < 13; n = 29, 20 males, mean age 9 ± 2 years) and age group 2 (13 ≤ years ≤ 18; n = 19, 14 males, mean age 15 ± 2 years) (**Table 1**). Comorbidities are detailed in **Table 2** and **Supplementary file 1**.

Table 1. Age and sex distribution of patients

Samples	#	Age group	Mean Age ± SD	Male sex %
Total	48	Whole cohort (6 ≤ years ≤ 18)	11 ± 4 years	71% (34 M and 14 F)
Stratified by age	29	1 (6 ≤ years < 13)	9 ± 2 years	69% (20 M and 9 F)
	19	2 (13 ≤ years ≤ 18)	15 ± 2 years	74% (14 M and 5 F)

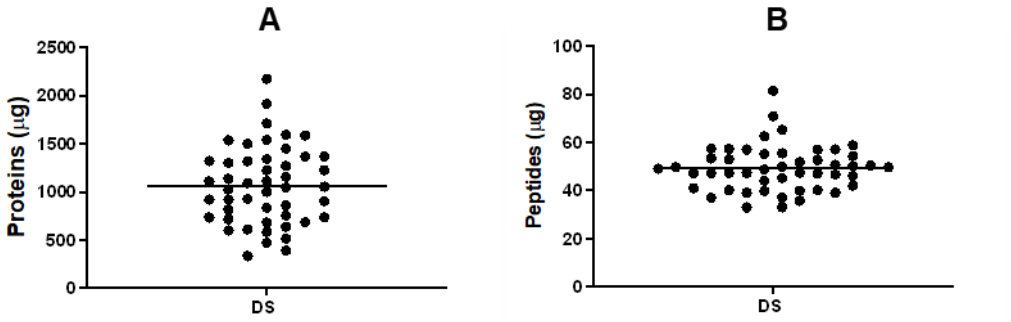
Table 2. Patients clinical features

Clinical variable	Whole cohort (6 ≤ years ≤ 18)	Age group	
		1 (6 ≤ years < 13)	2 (13 ≤ years ≤ 18)
	Cases N (frequency)		
Immunological disorders	28 (58%)	17 (59%)	11 (58%)
Alopecia	1 (2%)	1 (3%)	0 (0%)
Autoimmune thyroid disease (AITD)	20 (42%)	10 (34%)	10 (53%)
Celiac disease	8 (17%)	7 (24%)	1 (5%)
Recurrent respiratory infections	7 (15%)	6 (21%)	1 (5%)
Congenital heart diseases	11 (23%)	7 (24%)	4 (21%)
Hepatic steatosis or gastrointestinal tract disorders	6 (13%)	3 (10%)	3 (16%)
Nutritional disorders	13 (27%)	9 (31%)	4 (21%)
underweight: BMI < 5° percentile	4 (8%)	3 (10%)	1 (5%)
overweight: BMI between 85° and 95° percentile	8 (17%)	5 (17%)	3 (16%)
obese > 95°	1 (2%)	1 (3%)	0 (0%)
Behavioral disorders	24 (50%)	15 (52%)	9 (47%)
Internalizing problems (anxiety, depression, deflected mood, phobias)	7 (15%)	2 (7%)	5 (26%)
Externalizing problems (ADHD, ODD, emotional-behavioral and/or emotional dysregulation)	13 (27%)	9 (31%)	4 (21%)
Autism/social-relational and/or communicative impairments	5 (10%)	4 (14%)	1 (5%)

BMI: Body Mass Index; ADHD: attention-deficit hyperactivity disorder; ODD: oppositional defiant disorder

Fecal samples were subjected to a metaproteomic workflow to detect and quantify bacterial and host proteins. A total of 1,066 ± 406 µg of proteins were extracted (**Supplementary Figure 1A**) and enzymatic digestion of 50 µg of proteins yielded a mean value of 49.25 ± 9.53 µg of peptides. (**Supplementary Figure 1B**).

Supplementary Figure 1. Scatter plot graphs of quantified extracted proteins (panel A), and purified peptides (panel B). from stools of children with Down Syndrome (DS). Mean values are evidenced as black bar



The nLC-ESI-MS/MS procedure yielded a total of 124,370 PGs with 779,157 unique peptides sequences. Of these peptide sequences, 454,480 were assigned to a bacterial taxon by the LCA algorithm through Unipept. After filtering out PGs having fewer than 3 razor peptides, only PGs present in more than 50% of the entire sample set were retained, hence corresponding to 50,175 bacterial and 1,068 human PGs.

A statistically significant difference in sex proportions within the patient population was revealed by the binomial two-tailed test (p-value = 0.006). However, this disproportion had no impact on the overall composition of the GM metaproteome. Multivariate analyses were performed by stratifying the patient population based on sex, with 34 males and 14 females included in the study. Statistical analyses based on LFQ intensity values of identified PGs revealed no disparities, as evidenced by β-diversity metrics applied to the full LFQ PGs' matrix (bacteria + human PGs), and specifically to bacterial and human PGs (PERMANOVA test p-values = 0.126, 0.131, and 0.126, respectively). Furthermore, the PLS-DA analysis yielded no significance (p-value = 0.552, 0.710, and 0.775). Taken together, these results indicate that the unbalanced sex distribution of the cohort did not affect GM metaproteome composition, and that sex was therefore not a confounding factor in the subsequent analyses.

The metaproteome of GM in DS children was also analyzed according to age. The cohort was divided into two distinct groups. The first age group consists of 29 children aged between 6 and 12 years. The second age group consists of 19 children aged between 13 and 18 years (**Table 1**).

Upon patient stratification by age, β-diversity metrics applied to the entire LFQ PGs matrix or specifically to the bacterial and human PGs, revealed statistically significant differences

(PERMANOVA test p-value = 0.023, 0.027 and 0.041, respectively) (**Figure 1.A**). Moreover, PLS-DA revealed significant group separation exclusively based on human PGs (p-value = 0.025) (**Figure 1.C**). Overall, these results show that age, unlike sex, significantly influences the GM metaproteome composition of the whole DS pediatric population. The binomial two-tailed test revealed no statistically significant difference in sex proportions for both age groups (Age group 1: p-value = 0.062, and Age group 2: p-value = 0.064). Thus, the age-related differences described above cannot be ascribed to an uneven sex distribution between the two age groups.

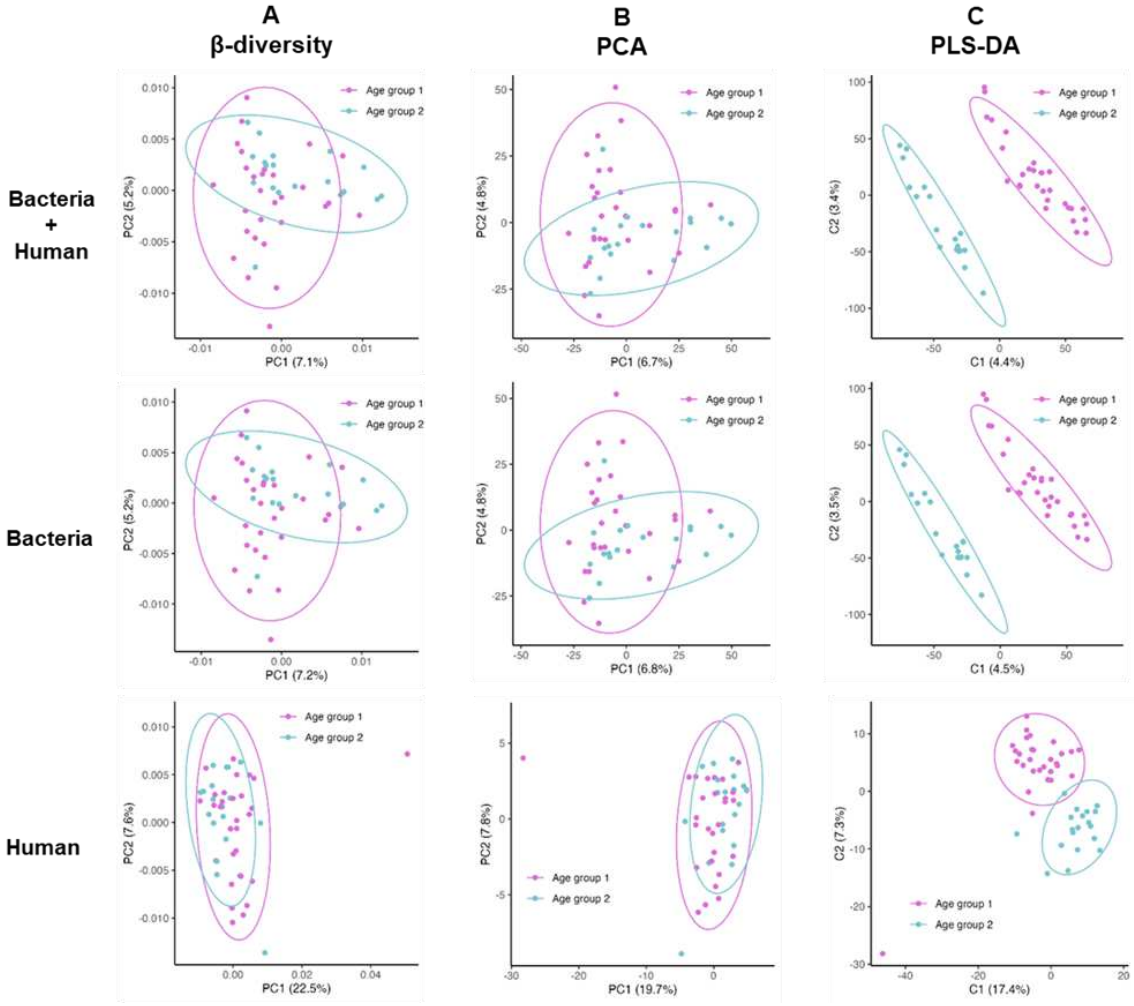


Figure 1. Analyses of quantified protein groups (PGs) from stool samples of children with Down syndrome stratified by their age: Age group 1, 6 ≤ years < 13, pink color, and Age group 2, 13 ≤ years ≤ 18, light blue color. The dissimilarity between the two groups was quantified using unsupervised Bray-Curtis β-diversity, based on their protein content (Panel A). The PERMANOVA test revealed statistically significant differences in the PG dataset, both when considering the entire matrix and when analyzing bacterial and host-derived PGs separately (bacterial and human PGs: *p*-value = 0.023; bacterial PGs: *p*-value = 0.027; human PGs: *p*-value = 0.041). Unsupervised Principal Component Analysis (PCA) displayed a separation amongst the two groups (Panel B). The Supervised Partial Least Squares-Discriminant Analysis (PLS-DA) model showed significance only considering the human PGs (bacterial and human PGs: *p*-value = 0.155; bacterial PGs: *p*-value = 0.154; human PGs: *p*-value = 0.025) (Panel C). The variances explained by each component are stated in brackets.

3.2 Comorbidities and patients' stratification

The following DS comorbidities were considered: A) presence of autoimmune thyroid diseases (AITDs); B) immune-related conditions, comprising the AITD cases considered in (A) as well as alopecia areata, celiac disease, and recurrent respiratory infections; C) behavioral disorders, comprising internalizing problems, such as anxiety, depression, deflected mood, and phobias, and externalizing problems, such as attention-deficit hyperactivity disorder (ADHD), oppositional defiant disorder (ODD), emotional-behavioral and/or emotional dysregulation; autism/social-relational and/or communicative impairments; and D) hepatic steatosis or gastrointestinal tract disorders and/or abnormal nutritional status.

Multivariate analyses based on clinical manifestations were performed on the whole dataset and within each age group (6–13 and 13–18 years). Beta-diversity applied to PG abundance distributions did not reveal any significant differences, regardless of whether the entire PG matrix, bacterial PGs, or human PGs were considered, and across both age groups (**Supplementary file 2**). Similarly, PLS-DA indicated no significant differences (**Supplementary file 2**).

Supplementary file 2. Beta-diversity and PLS-DA statistical outputs stratified by age group and clinical features

Age group		Comparison	Analysis	Bacterial + human PGs	Bacterial PGs	Human PGs	# subjects		
				p-value	*p*-value	*p*-value	Yes (or Age group 1)	No (or Age group 2)	Total
Age group 1 and 2 (6 ≤ years ≤ 18)	A	Autoimmune thyroid diseases (AITDs) yes *vs* no	Beta Diversity	0.690	0.705	0.072	20	28	48
			PLSDA	0.664	0.758	0.221			
	B	Immunological diseases yes *vs* no	Beta Diversity	0.609	0.6	0.949	28	20	48
			PLSDA	0.594	0.656	0.916			
	C	Behavioral disorders yes *vs* no	Beta Diversity	0.314	0.322	0.482	24	23	47
			PLSDA	0.294	0.317	0.437			
	D	Hepatic steatosis or gastrointestinal tract disorders and/or nutritional disorders yes *vs* no	Beta Diversity	0.311	0.346	0.180	15	33	48
			PLSDA	0.165	0.563	0.508			
Age group 1 (6 ≤ years < 13)	A	AITDs yes *vs* no	Beta Diversity	0.973	0.981	0.537	10	19	29
			PLSDA	0.794	0.919	0.669			
	B	Immunological diseases yes *vs* no	Beta Diversity	0.331	0.338	0.659	17	12	29
			PLSDA	0.597	0.620	0.603			
	C	Behavioral disorders yes *vs* no	Beta Diversity	0.253	0.251	0.572	15	13	28
			PLSDA	0.473	0.367	0.407			
	D	Hepatic steatosis or gastrointestinal tract disorders and/or nutritional disorders yes *vs* no	Beta Diversity	0.567	0.582	0.212	10	19	29
			PLSDA	0.353	0.484	0.162			
Age group 2 (13 ≤ years ≤ 18)	A	AITDs yes *vs* no	Beta Diversity	0.506	0.516	0.125	10	9	19
			PLSDA	0.542	0.579	0.240			
	B	Immunological diseases yes *vs* no	Beta Diversity	0.472	0.508	0.153	11	8	19
			PLSDA	0.574	0.583	0.192			
	C	Behavioral disorders yes *vs* no	Beta Diversity	0.449	0.425	0.621	9	10	19
			PLSDA	0.480	0.317	0.586			
	D	Hepatic steatosis or gastrointestinal tract disorders and/or nutritional disorders yes *vs* no	Beta Diversity	0.592	0.565	0.472	5	14	19
			PLSDA	0.928	0.928	0.768			

3.3 Influence of clinical traits on the GM metaproteome of children with DS

To complement multivariate findings, a univariate analysis was performed to investigate GM metaproteome modulation based on clinical features, stratifying subjects by age group.

A mean of 911 ± 236 differentially expressed PGs were identified depending on the diverse stratification strategies (**Supplementary file 3**). We acknowledged that the sample size for comparisons involving clinical features of group C (hepatic steatosis or gastrointestinal disorders and/or abnormal nutritional status), was imbalanced in age group 2 (14 subjects vs. 5). Therefore, the result of this comparison was not presented, discussed, or analyzed for either age group.

Supplementary file 3. Number of differentially expressed protein groups (PGs) and their regulation trend (up: over-expression; down: under-expression) based on clinical traits groupings

Age group		Comparison	Univariate Analysis									# subjects		
			# differentially expressed PGs											
			Bacterial + Human			Bacterial			Human			Yes	No	Total
			total	up	down	total	up	down	total	up	down			
Age group 1 (6 ≤ years < 13)	A	Autoimmune thyroid diseases (AITDs) yes *vs* no	544	316	228	532	314	218	12	2	10	10	19	29
	B	Immunological diseases yes *vs* no	735	379	356	720	365	355	15	14	1	17	12	29
	C	Behavioral disorders yes *vs* no	780	247	533	771	245	526	9	2	7	15	13	28
	D	Hepatic steatosis or gastrointestinal tract disorders and/or nutritional disorders yes *vs* no	800	461	339	767	460	307	33	1	32	10	19	29
Age group 2 (13 ≤ years ≤ 18)	A	AITDs yes *vs* no	1112	392	720	1091	391	700	21	1	21	10	9	19
	B	Immunological diseases yes *vs* no	1004	308	696	986	307	679	18	1	17	11	8	19
	C	Behavioral disorders yes *vs* no	1042	534	508	1022	525	497	20	9	11	9	10	19
	D	Hepatic steatosis or gastrointestinal tract disorders and/or nutritional disorders yes *vs* no	1271	496	775	1245	478	767	26	18	8	5	14	19

The presence of AITDs had an impact on 544 PGs in age group 1 and on 1,112 PGs in age group 2. Of these PGs, 532 and 1,091 respectively, were of bacterial origin. Among these the differentially abundant bacterial PGs, 487 and 987 had an assigned COG name, 249 and 555 a KEGG pathway name, resulting in a total of 348 and 547 different COG names, 23 and 22 COG categories (**Figure 2A**), and 112 and 123 KEGG pathways, respectively. In addition, the LCA algorithm assigned a taxon

to 517 PGs and 1069 for a total of 188 and 260 unique taxa, respectively (**Table 3** and **Supplementary File 3**).

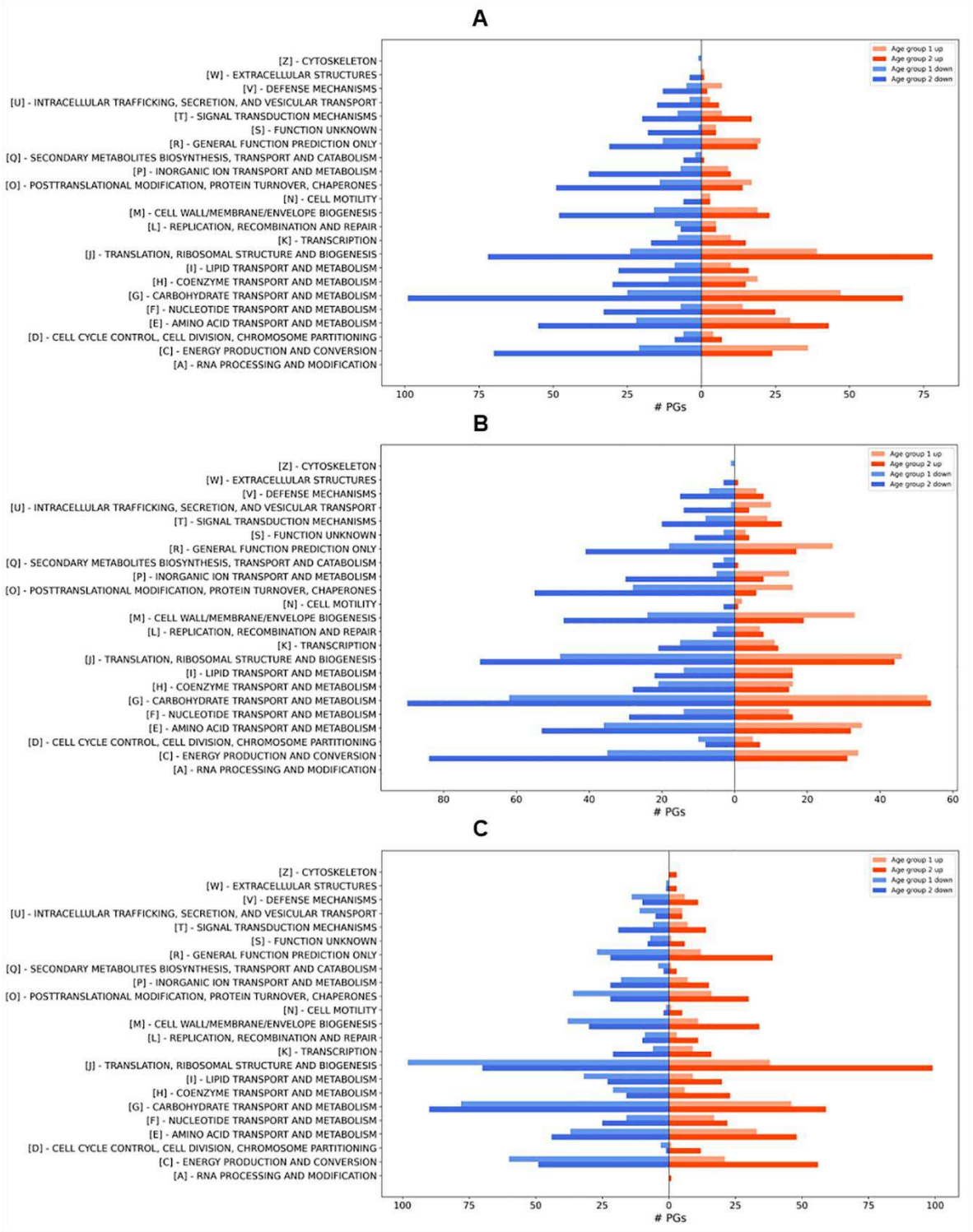


Figure 2. Graphical representation of COG categories modulated in differentially expressed bacterial protein groups (PGs) comparing DS subjects with or without A. thyroid diseases, B. immunological diseases, and C. behavioral disorders. The bars represent the frequency of differentially expressed bacterial PGs associated with their functional annotation. The color coding of orange (on the right side of the bar) and blue (on the left side of the bar) denotes over-expressed (up) and under-expressed (down) PGs in the presence of the diseases/disorders, respectively. The two shades of color represent the different age groups: lighter colors indicate age group 1 and darker colors indicate age group 2.

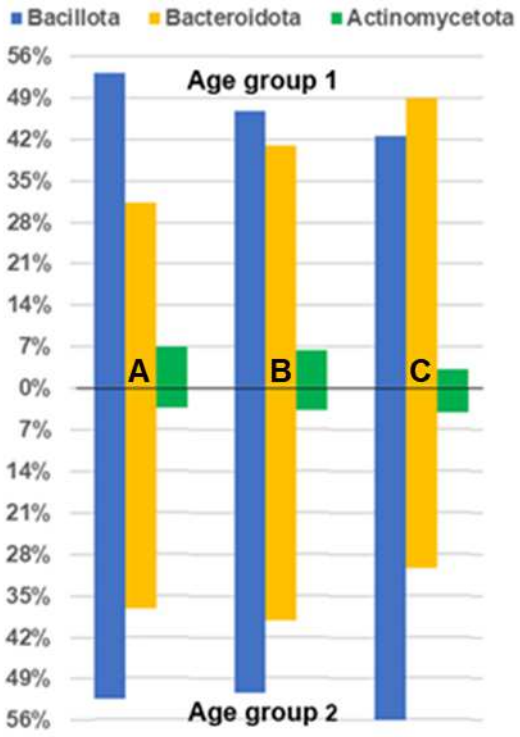
Table 3. Results of the univariate analysis of the fecal metaproteome in terms of the number of both differentially expressed bacterial protein groups (PGs) and their associated functional and taxonomic annotation across the three comorbidity comparisons and the two age groups

Variable	Comparison											
	A. Autoimmune thyroid diseases yes *vs* no				B. Immunological diseases yes *vs* no				C. Behavioral disorders yes *vs* no			
Age group	**1**		**2**		**1**		**2**		**1**		**2**	
# bacterial PGs	532		1091		720		986		771		1022	
# PG with assigned COG name	487	91.54%	987	90.47%	661	91.81%	893	90.57%	726	94.16%	958	93.74%
# total different COG names	348	65.41%	547	50.14%	420	58.33%	531	53.85%	415	53.83%	536	52.45%
# total COG categories	23		22		22		22		21		24	
# PGs with assigned KEGG pathway	249	46.80%	555	50.87%	365	50.69%	504	51.12%	410	53.18%	528	51.66%
# total KEGG pathways	112		123		115		123		122		120	
# PGs with assigned taxon by LCA	517	97.18%	1069	97.98%	705	97.92%	973	98.68%	759	98.44%	1000	97.85%
# different taxa by LCA	188		260		204		238		200		238	
# PGs assigned to Bacillota phylum	283	53.20%	573	52.52%	336	46.67%	508	51.52%	328	42.54%	581	56.85%
# PGs assigned to Bacteroidota phylum	167	31.39%	406	37.21%	295	40.97%	387	39.25%	378	49.03%	312	30.53%
# PGs assigned to Actinomycetota phylum	37	6.95%	37	3.39%	46	6.39%	38	3.85%	25	3.24%	43	4.21%
# PGs assigned to Pseudomonadota phylum	15	2.82%	20	1.83%	16	2.22%	21	2.13%	21	2.72%	25	2.45%
# PGs assigned to Verrucomicrobiota phylum	10	1.88%	17	1.56%	3	0.42%	5	0.51%	4	0.52%	33	3.23%
# PGs assigned to other phyla	5	0.94%	16	1.47%	9	1.25%	14	1.42%	3	0.39%	6	0.59%

In age group 1, 283 PGs (53.20%) of the differentially expressed bacterial PGs were assigned to the Bacillota phylum (formerly Firmicutes), with Lachnospiraceae (114 PGs), Oscillospiraceae (74 PGs), Veillonellaceae (18 PGs), and Acidaminococcaceae (12 PGs) families being prevalent. Bacteroidota or Bacteroidetes accounted for 31.39% of the differentially expressed PGs (167 PGs), while Actinomycetota or Actinobacteria accounted for 6.95% (37 PGs), Pseudomonadota (formerly Proteobacteria) accounted for 2.82% (15 PGs), and Verrucomicrobiota (formerly Verrucomicrobia) accounted for 1.88% (10 PGs). In age group 2, the most represented phylum was also the Bacillota, accounting for 574 differentially expressed PGs (52.61%), with Lachnospiraceae (150 PGs), Oscillospiraceae (163 PGs), Veillonellaceae (29 PGs), and Erysipelotrichaceae (24 PGs) families being prevalent.

As demonstrated in **Table 3**, the numerical values associated with the two additional comparisons (presence *vs* absence of [B] immunological-related diseases or [C] behavioral disorders), were analogous. Out of a mean of 854 ± 215 bacterial differentially expressed PGs among the six comparisons (two age groups and three clinical stratifications), 91.62% ± 1.57% of PGs were assigned a COG name, 50.23% ± 2.12% PGS were assigned a KEGG pathway, and 97.92% ± 0.52% PGs were assigned a taxon by LCA. At the phylum level, the percentages were as follows: Bacillota (52.15% ± 5.11%), Bacteroidota (35.87% ± 6.81%), Actinomycetota (4.96% ± 1.60%), Pseudomonadota (2.29% ± 0.37%), and Verrucomicrobiota (1.52% ± 1.11%). The primary distinction can be ascribed to the differential expression of PGs in the presence of behavioral disorders in subjects with an age below 13 years (age group 1). In this instance, the predominant phylum was Bacteroidota, superseding

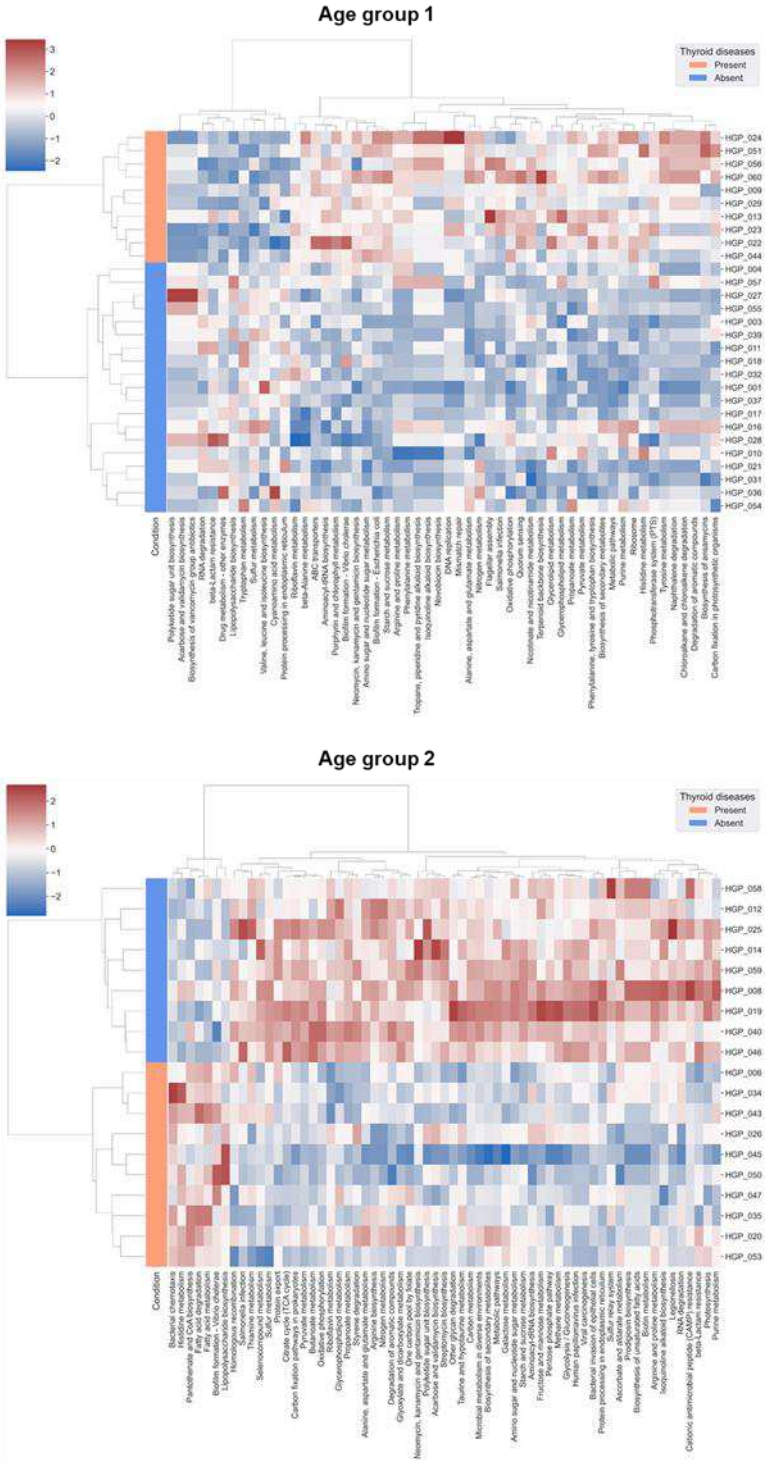
Bacillota, albeit by a marginal margin (49.03% *vs* 42.54%) (**Supplementary File 3** and **Supplementary Figure 2**).



Supplementary Figure 2. Relative distribution (%) of the three major phyla associated with differentially expressed Protein Groups across three stratification strategies: (A) presence/absence of autoimmune thyroid disease; (B) immunological diseases; and (C) behavioral disorders. Upper and lower panels represent age group 1 and age group 2, respectively.

In an effort to identify functional characteristics of the microbiota that could be associated with the three clinical outcomes, a more in-depth assessment of the modified pathways was conducted. Among the KEGG pathways associated with the identified bacterial PGs, statistically significant differences were found for 62 ± 12 pathways, among the six comparisons (**Supplementary File 4**).

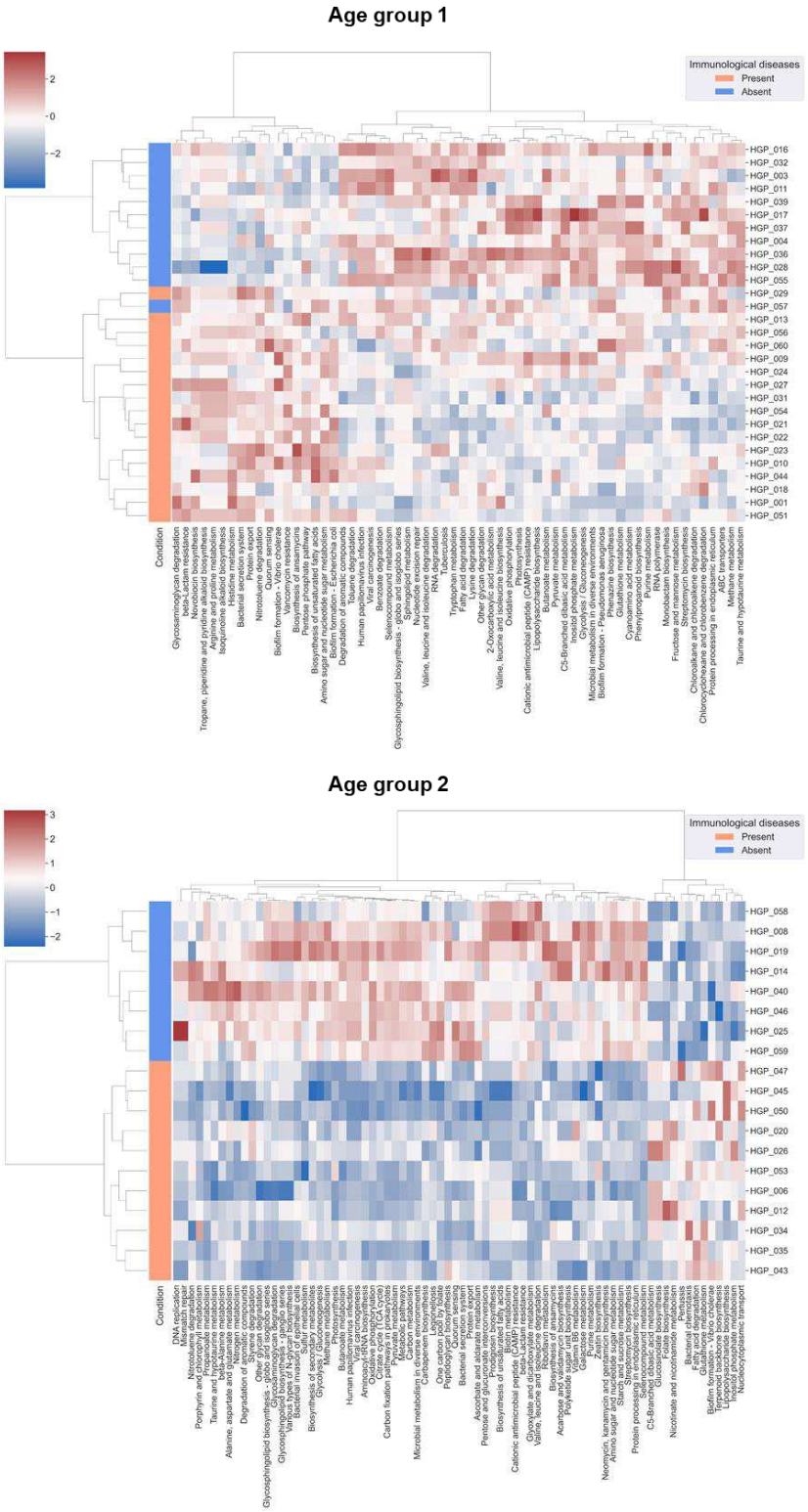
The presence of AITDs diseases had a significant impact on 54 KEGG pathways for age group 1 and 63 for age group 2 (**Supplementary File 4** and **Supplementary Figure 3**).



Supplementary Figure 3. Cluster analyses were conducted on differentially expressed KEGG pathways that were associated with the identified bacterial protein groups (PGs) found in stool samples from patients with DS with or without autoimmune thyroid diseases. The color coding of orange and blue denotes over-expressed and under-expressed KEGG pathways in the presence of the diseases/disorders, respectively. The mean intensity abundance of PGs with the same KEGG pathways for each sample was calculated. Statistically significant pathways were then identified by computing a Mann-Whitney test and adjusted *p*-value for false discovery rate (using Benjamini-Hochberg correction for independent or positively correlated tests). For the number of KEGG pathways, their regulation, and associations with PGs, please refer to the Supplementary File 4.

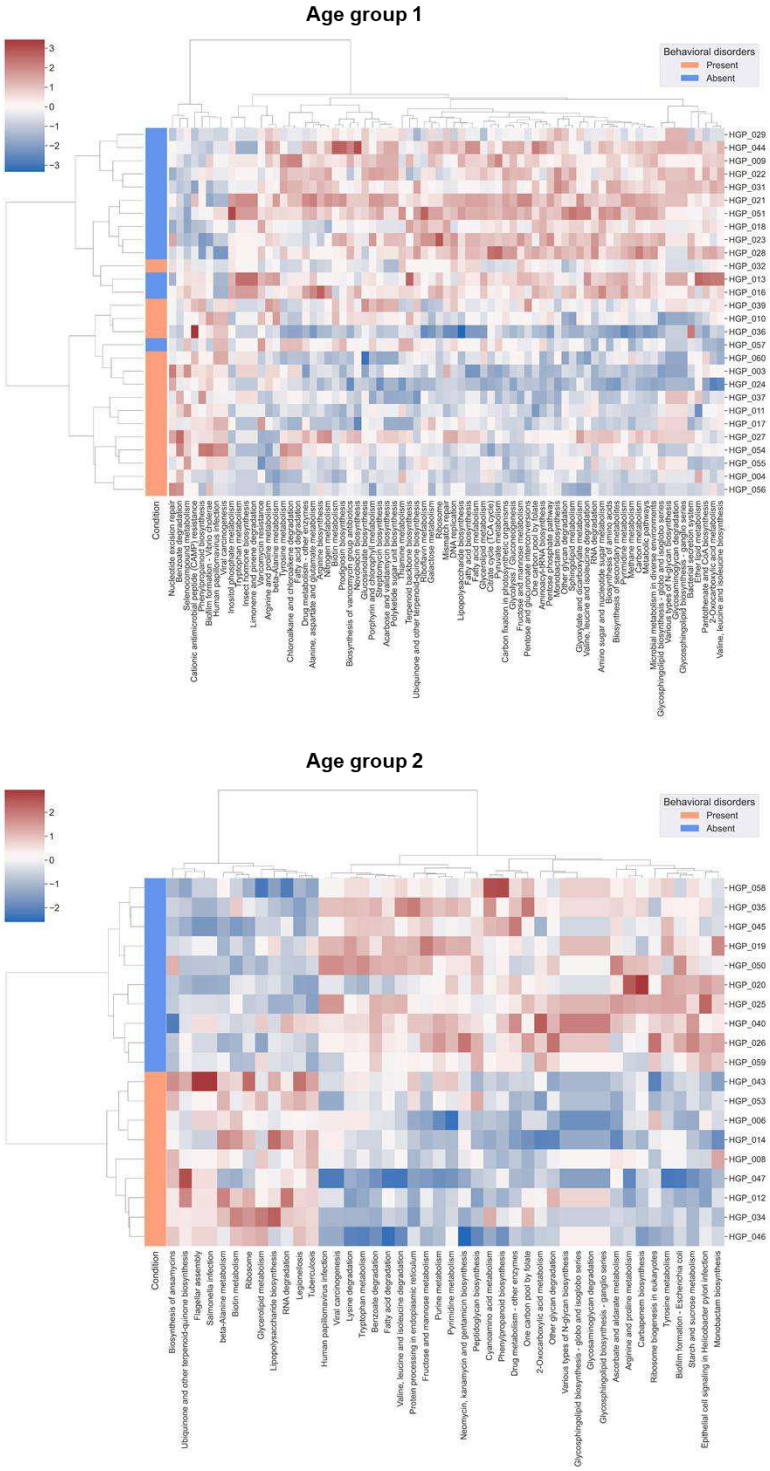
Among these pathways, six were found to be common, exhibiting the same regulatory pattern; one (Histidine metabolism) was found to be over-expressed, and five were found to be under-expressed (**Figure 3A**). Among the latter, RNA degradation and beta-Lactam resistance are those associated with the highest number of differentially expressed PGs: 8 and 6 for age group 1, and 28 and 8 for age group 2, respectively.

The presence of immunological diseases had an effect on 62 KEGG pathways in age group 1 and 76 KEGG pathways in age group 2 (**Supplementary File 4** and **Supplementary Figure 4**).



Supplementary Figure 4. Cluster analyses were conducted on differentially expressed KEGG pathways that were associated with the identified bacterial protein groups (PGs) found in stool samples from patients with DS with or without immune-related comorbidities. The color coding of orange and blue denotes over-expressed and under-expressed KEGG pathways in the presence of the diseases/disorders, respectively. The mean intensity abundance of PGs with the same KEGG pathways for each sample was calculated. Statistically significant pathways were then identified by computing a Mann-Whitney test and adjusted *p*-value for false discovery rate (using Benjamini-Hochberg correction for independent or positively correlated tests). For the number of KEGG pathways, their regulation, and associations with PGs, please refer to the Supplementary File 4.

Behavioral diseases were associated with 75 and 44 KEGG pathways, respectively (**Supplementary File 4** and **Supplementary Figure 5**).



Supplementary Figure 5. Cluster analyses were conducted on differentially expressed KEGG pathways that were associated with the identified bacterial protein groups (PGs) found in stool samples from patients with DS with or without immune-related comorbidities. The color coding of orange and blue denotes over-expressed and under-expressed KEGG pathways in the presence of the diseases/disorders, respectively. The mean intensity abundance of PGs with the same KEGG pathways for each sample was calculated. Statistically significant pathways were then identified by computing a Mann-Whitney test and adjusted *p*-value for false discovery rate (using Benjamini-Hochberg correction for independent or positively correlated tests). For the number of KEGG pathways, their regulation, and associations with PGs, please refer to the Supplementary File 4.

We focused on KEGG pathways that were consistently altered in both age groups. The number of common modulated pathways in the presence of immunological diseases or behavioral disorders was higher than in the AITD based comparison, reaching 15 **(Figure 3B**) and 16 (**Figure 4**), respectively, with a consistently negative regulation trend. Among all comparisons, the immunological disease-based comparison yielded the pathway with the highest number of differentially expressed PGs (86 PGs for age group 1 and 137 for age group 2). This pathway, Microbial metabolism in diverse environments, was also the broadest, as it encompassed several more specific pathways, such as Glycolysis/Gluconeogenesis, Methane metabolism, Purine metabolism, and Pyruvate metabolism. These pathways were also among those commonly modulated in both age groups, with a high number of differentially expressed PGs (Glycolysis/Gluconeogenesis: 39 and 59; Methane metabolism: 15 and 25; Purine metabolism: 22 and 56; Pyruvate metabolism: 27 and 50, for age group 1 and age group 2, respectively). The Butanoate metabolism was likewise among the most represented pathways, with a large number of enzymes mapped across nearly all reaction steps (11 and 24 PGs for age group 1 and age group 2, respectively, spanning the central acetyl-CoA route to butyrate as well as the succinate/γ-aminobutyric acid [GABA] branch, **Figure 5**).

In the presence of behavioral disorders, a total of 75 KEGG pathways were modulated in age group 1 and 44 in age group 2 (**Supplementary File 4**), with 16 shared pathways identified across both age groups. The most represented pathways were 2-oxocarboxylic acid metabolism (7 and 12 PGs for age group 1 and age group 2, respectively), Fructose and mannose metabolism (21 PGs in both age groups), Pyrimidine metabolism (23 and 40 PGs, respectively), and Valine, leucine, and isoleucine degradation (7 and 9 PGs, respectively).

Interestingly, the two age groups shared no or very few PGs (0, 2, and 1, respectively, for the three comparisons) associated with the commonly modulated KEGG pathways. Furthermore, no shared KEGG pathways were identified across the three comparisons and both age groups. Only three modulated KEGG pathways were shared in the presence of immunological and behavioral disorders, namely Glycosphingolipid biosynthesis – globo and isoglobo series, Other glycan degradation, and Valine, leucine and isoleucine degradation.

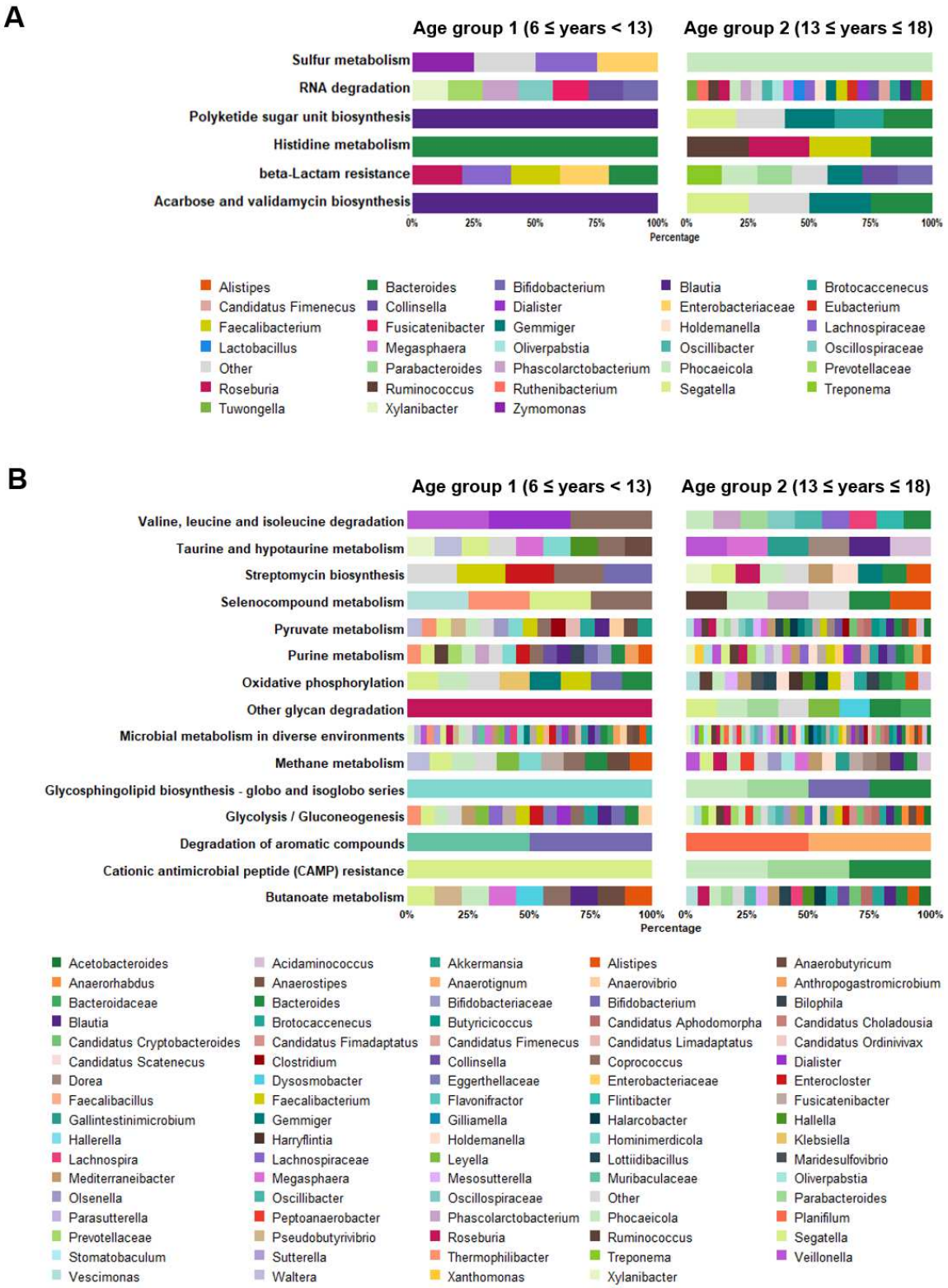


Figure 3. Lowest common ancestor (LCA) taxonomic distribution of the differentially expressed bacterial Protein Groups (PGs) within the KEGG pathways differentially modulated in the same direction in both age groups, comparing DS subjects with and without immune-related conditions: (A) autoimmune thyroid diseases (AITDs) specifically, and (B) any immune system disorder, including the AITDs considered in (A). Stacked bars report the percentage contribution of

each LCA taxon, annotated at genus level or, where assignment was not resolved further, at family level; PGs whose LCA was resolved only at higher taxonomic ranks (order or above) are grouped as “Other”.

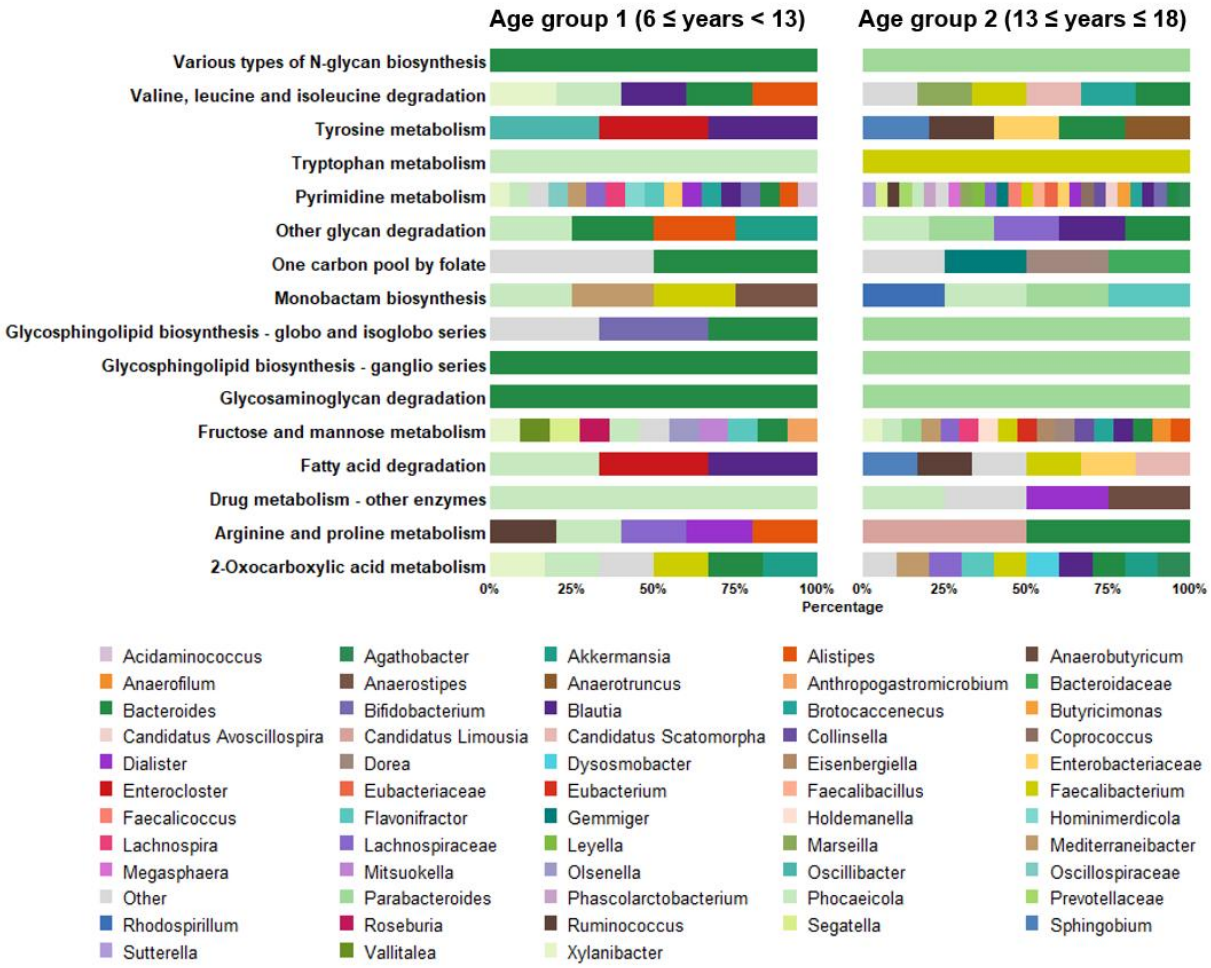


Figure 4. Lowest common ancestor (LCA) taxonomic distribution of the differentially expressed bacterial Protein Groups (PGs) within the KEGG pathways differentially modulated in the same direction in both age groups, comparing DS subjects with and without behavioral disorders. Stacked bars report the percentage contribution of each LCA taxon,

annotated at genus level or, where assignment was not resolved further, at family level; PGs whose LCA was resolved only at higher taxonomic ranks (order or above) are grouped as "Other".

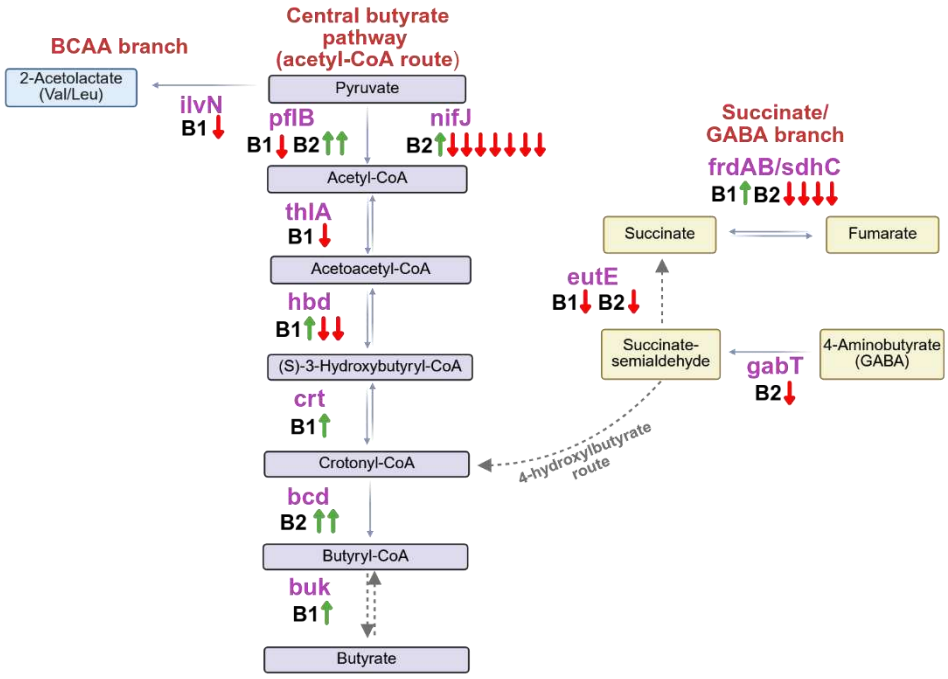


Figure 5. Butanoate metabolism exploited by bacterial differentially expressed Protein groups (PGs) in children with DS of age group 1 (B1, 6 ≤ years < 13) and age group 2 (B2, 13 ≤ years ≤ 18) in presence of immunological diseases, and detected along the butyrate biosynthesis pathway, the succinate/γ-aminobutyric acid branch (GABA), and Branched-chain amino acid (BCAA) branch. Metabolites are shown in boxes and each reaction step is labelled with the gene name of PG(s) assigned to it. Each arrow corresponds to one PG; green/red arrows indicate up-/down-expression ($\log_{10}FC \geq |0.3|$). PGs are labelled with gene name: pflB, formate acetyltransferase; nifJ, pyruvate synthase; thlA, acetyl-CoA acetyltransferase; hbd, 3-hydroxybutyryl-CoA dehydrogenase; crt, short-chain enoyl-CoA hydratase; bcd, short-chain acyl-CoA dehydrogenase; buk, butyrate kinase; ilvN, acetolactate synthase small subunit; frdA, fumarate reductase flavoprotein subunit; frdB, fumarate reductase iron–sulfur subunit; sdhC, succinate dehydrogenase cytochrome b subunit; eutE, acylating succinate-semialdehyde dehydrogenase; gabT, 4-aminobutyrate aminotransferase. Double-headed solid arrows denote reversible single-step reactions; dashed arrows denote transitions in which o.ne or more additional enzymatic steps occur between the two metabolites shown. Created with BioRender.com.

3.4 Protein groups of human origin

A total of 79 differentially expressed human PGs were identified across the different comparisons. Of these, 80% (63 PGs) were specific to a single age group and stratification type, while 16 were shared across at least one of the six comparisons (**Supplementary File 5**). Specifically, the largest number of shared PGs (12) was identified for age group 2 across two comparisons: presence or absence of AITDs (A.2) and presence or absence of immunological disease (B.2, which includes A.2). Notably, the majority of human PGs showing differential regulation were under-expressed in the presence of the considered comorbidities (mean of 11 ± 7 under-expressed PGs out of a total of 16 ± 5 PGs). However, this trend was not observed in B.1, where 14 out of 15 differentially expressed PGs were over-expressed.

As expected, the most represented Gene Ontology (GO) Cellular Component (CC) terms associated with the 79 differentially expressed human PGs were the extracellular space (GO:0005615) and

extracellular region (GO:0005576) based on PANTHER Overrepresentation CC-Slim Test (17 PGs respect to the Reference List = all genes in the human database, *p*-value = 4.94 x 10^{-4} and 9.23 x 10^{-4}, respectively) (**Supplementary File 5**). Indeed, when each list of differentially expressed human PGs was analyzed separately using the FunRich application, the following GO CC terms were identified as the most populated: extracellular space, cytoplasm, extracellular vesicular exosome, and plasma membrane. Of these terms, extracellular vesicular exosome was the term that was significantly over-represented in three comparisons (**Figure 6** and **Supplementary File 5**).

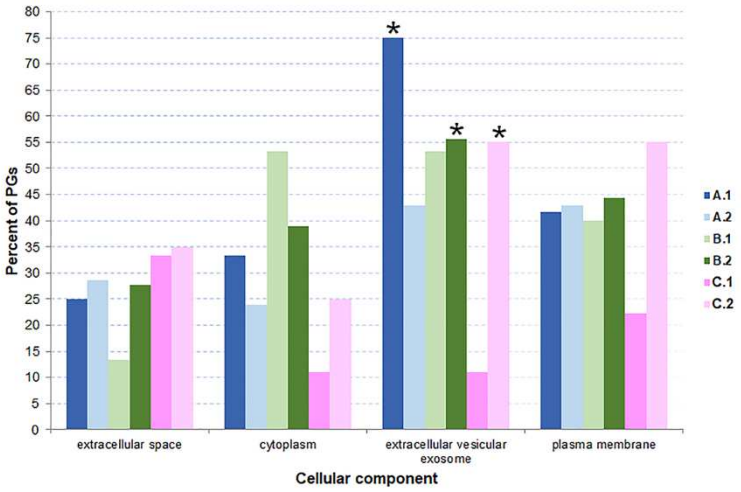


Figure 6. Graphical representation of the distribution of the most populated Gene Ontology Cellular Component terms among the six comparisons by the FunRich application. A = autoimmune thyroid diseases, B = immunological diseases, and C = behavioral disorders. 1 = age group 1 (6 ≤ years < 13) and 2 = age group 2 (13 ≤ years ≤ 18). * = *p*-value < 0.05 (Bonferroni correction) of enrichment comparing the identified protein list to expected occurrence in the whole human proteome. Specifically, the *p*-values were determined to be 7.20 × 10^{-04} for A.1, 9.31 × 10^{-03} for B.2, and 3.52 × 10^{-03} for C.2.

Eighteen out of 79 human PGs contributed to the over-representation of two GO molecular function (MF) terms: antigen binding (GO:0003823, five PGs, PANTHER MF-Slim *p*-value = 3.43 × 10^{-2}) and hydrolase activity (GO:0016787, 16 PGs, *p*-value = 4.05 × 10^{-2}) (**Supplementary File 5**). With respect to the GO Biological process (BP) terms, 15 human PGs contributed to an over-representation of production of molecular mediator of immune response (GO:0002440, 6 PGs, PANTHER BP-Slim *p*-value = 3.44 × 10^{-3}), its child node immune system process (GO:0002376, 14 PGs, *p*-value = 6.68 × 10^{-5}), and immune response (GO:0006955, 12 PGs, *p*-value = 3.28 × 10^{-4}) (**Supplementary File 5**).

Reactome Pathway Analysis enabled us to identify enriched pathways, providing key biological insights for each of the six datasets (**Supplementary File 6**). Although no pathway modulations were identical across all datasets, with the exception of two Mesenchymal-Epithelial Transition factor (MET)-related pathways, several recurring biological themes emerged, including extracellular matrix (ECM) remodeling (e.g., Collagen biosynthesis and modifying enzymes, Collagen chain trimerization, Collagen degradation, ECM proteoglycans, Fibronectin matrix formation), scavenger

receptor-mediated ligand binding and uptake (e.g., Binding and Uptake of Ligands by Scavenger Receptors, Scavenging by Class A Receptors), and glucose metabolism dysregulation (e.g., Gluconeogenesis, Glucose metabolism). Additional shared motifs involved cell motility and signaling via MET (e.g., MET activates PTK2 signaling, MET promotes cell motility, Signaling by MET) and NCAM/Integrin interactions (e.g., Immunoregulatory interactions between a Lymphoid and a non-Lymphoid cell, Integrin cell surface interactions, NCAM signaling for neurite out-growth, NCAM1 interactions, Syndecan interactions).

4 Discussion

Children diagnosed with DS frequently exhibit diminished immune function and cognitive performance, and an augmented vulnerability to health complications in comparison to their typically developing peers. As life expectancy in DS has increased, so too has the prevalence of age-associated conditions, including AD, infections, hypertension, obesity, and notably GI disorders, which can strongly affect daily functioning. Evidence also indicates that individuals with DS have a higher propensity for autoimmune conditions and respiratory infections, pointing to possible deficiencies in humoral immunity. It is hypothesized that disruptions in microbial communities may contribute to both the GI issues and immune impairments observed in DS, given the critical role of the GM in regulating immune responses and maintaining physiological balance. Indeed, the concept of leveraging the microbiota-gut-brain axis to manage DS and other pediatric neurodevelopmental disorders is an intriguing one [27]. However, the absence of robust translational insights is still hindering the transformation of this concept into a strategic approach. The present paper aims to contribute to the existing body of knowledge by offering insights into GM's distinctive microbial and functional patterns related to the different clinical manifestations of DS. The metaproteomic survey of the GM in children with Down syndrome stratified by comorbidity conducted in this study complemented existing Down syndrome work, which has relied largely on 16S-based composition [10, 12, 13], shotgun metagenomics in twins discordant for T21 [28], or fecal metabolomics [11].
We acknowledge that interindividual variations and the modest sample size imply that our findings are not especially robust. Therefore, it will be crucial to validate the results on a larger cohort while also accounting for the GM metaproteome of healthy subjects to better understand at functional level the differences between them and children with DS, as described by other studies based on metagenomic and metabolomic approaches (**Supplementary file 7**) [28, 13, 11, 12, 29, 10]. Notwithstanding, the present study is deemed pertinent for two primary reasons. The first is intrinsic to the approach used, namely metaproteomics, which enabled the description of the actual proteins present in the GM and, consequently, its functionality. Indeed, the pathogenesis of T21 disrupts

numerous metabolic pathways. These disruptions warrant comprehensive evaluation through omics-based approaches, particularly metaproteomics, which could yield valuable insights into functional protein dysregulation and potential therapeutic targets. Unlike metagenomics that reveals only microbial genetic potential without insights into actual activity, metaproteomics provides direct functional information by identifying and quantifying proteins that actively participate in metabolic pathways, thereby elucidating which pathways are genuinely operational rather than merely inferring them from genetic sequences [30, 31]. As noted by previous researchers, there remains a critical need to characterize the metabolic pathway deficiencies underlying T21 pathomechanisms, with bioinformatics enabling the integration of multi-omics and clinical data for meaningful interpretation [32].

Furthermore, this paper's investigation revealed that, even in the context of DS, the GM exhibited a modulation according to age, as is the case in healthy children and unlike other genetic diseases such as Williams syndrome [33]. As known, microbiome undergoes modulation from birth to senescence, experiencing significant changes during early life, and appearing to stabilize in healthy adults with infant-adult trajectories [14, 15]. However, it is important to note that this physiological modulation may not be present in pathological conditions. Therefore, its presence or absence should be verified on a case-by-case basis.

Starting from the evidence that the GM metaproteome is different between the 2-age range of our cohort, we stratified children with DS first by age and then by clinical symptoms. We hypothesize that the GM acts as a modulator of the host phenotype and therefore represents a promising target for patient stratification and for managing DS comorbidities and behavioral features. Consequently, the GM modulation was evaluated based on clinical metadata. Despite the broad spectrum of clinical comorbidities captured in the metadata, univariate analyses were restricted to three stratification strategies, selected on the basis of their ability to ensure an adequate and balanced sample size across comparisons. In particular, we analyzed the effect of the presence or absence of the following: AITDs diseases (A), immunological-related diseases, including AITDs (B), and behavioral disorders (C).

Thyroid pathology represents one of the most prevalent and clinically significant complications in individuals with Down syndrome, with lifetime thyroid dysfunction incidence approaching 63% in DS populations, substantially exceeding rates observed in the general population [34]. Congenital hypothyroidism affects approximately 1% of DS newborns, while thyroid function test abnormalities are documented in over 50% of DS [4, 5]. The progressive nature of thyroid disease is particularly noteworthy, with approximately 50% of DS individuals developing thyroid abnormalities including persistent hypothyroidism and autoimmune thyroiditis by age 45 years [5]. Autoimmune mechanisms represent the predominant pathogenic pathway for thyroid dysfunction in DS. Autoimmune thyroid

disease, confirmed by positive thyroid autoantibodies, occurs in 13-34% of DS individuals compared to only 3% in the general population [35] with Hashimoto's thyroiditis constituting the most frequently diagnosed condition. Timely identification and therapeutic intervention can substantially reduce long-term complications affecting growth, cognitive development, and metabolic function [5]. The elevated prevalence of AITDs in DS population reflects generalized immune system dysfunction rather than isolated endocrine abnormality. Approximately one-third of individuals with DS develop autoimmune disorders, with the concurrent presence of heightened autoimmune disease rates and increased vulnerability to infections, particularly respiratory tract infections, pointing toward fundamental immune dysregulation [35]. Beyond thyroid disease, celiac disease affects 5-7% of DS individuals versus 0.5-2% of neurotypical populations [35, 36]. Type 1 diabetes mellitus, alopecia areata, Addison's disease, and juvenile idiopathic arthritis all occur with greater frequency in DS compared to age-matched neurotypical populations [4, 5]. One possible explanation is based on the evidence that chromosome 21 encodes four interferon receptor genes whose triplication leads to constitutive interferon pathway activation [37]. Indeed, this constitutive type I interferonopathy predisposes to multiple autoimmune conditions including AITDs [38, 39]. Murine models demonstrate that interferon receptor triplication is causally linked to multiple DS phenotypes, with normalization of copy number ameliorating autoimmune manifestations [40].

Accumulating data have shown that DS is characterized by constitutional predisposition to autoimmune disease development, wherein chronic cytokine dysregulation, aberrant CD4 T lymphocyte activation, and sustained B cell activity collectively promote loss of immune tolerance [41]. As life expectancy for DS individuals continues to increase, understanding and managing thyroid and autoimmune diseases becomes progressively more important for optimizing quality of life. Indeed, DS is classically defined as a neurodevelopmental disorder, yet mounting evidence highlights a systemic immune dimension marked by chronic inflammation and susceptibility to autoimmunity. From an innate immunity standpoint, DS shares core features with interferon-driven, autoinflammation-like conditions [42]. Recognition of DS as involving fundamental immune dysregulation presents therapeutic opportunities through immunomodulatory agents, while mechanistic insights may inform understanding of autoimmune disorders more broadly [5, 41]. Despite DS being one of the most common genetic conditions, the immune dysregulation associated with it remains largely underrecognized and understudied, notwithstanding its significant contribution to morbidity and mortality in affected individuals [43].

Our finding of a downregulation of bacterial sulfur metabolism in AITDs in both age groups of DS children is noteworthy due to its ties to neurological conditions and the known link to brain health and neurological diseases [44]. Microbial sulfur metabolism encompasses the production of hydrogen

sulfide (H_2S), a gasotransmitter with proposed anti-inflammatory and immunomodulatory properties [45]. H_2S produced by the GM significantly contributes to the total sulfide burden in the body whose effects on the intestinal environment are concentration-dependent: at high concentrations it can compromise the mucus barrier, impair epithelial integrity, and promote inflammation whereas at physiological levels it exerts anti-inflammatory and cytoprotective properties, stabilizing microbial biofilms and preventing pathogenic colonization [46]. In DS specifically, transcriptomic and proteomic evidence points to H_2S overproduction in white blood cells driven not by the canonical cystathionine-β-synthase (CBS) pathway, as previously assumed being CBS an Hsa21-resident gene whose overexpression had long been considered the primary driver of H_2S excess in DS, but through a noncanonical thioredoxin- and MPST-dependent cysteine catabolism route, tightly coupled to elevated SOD1 expression and oxidative stress [47]. This endogenous H_2S excess coexists with upregulated sulfide-oxidizing enzymes (SQOR, ETHE1), suggesting a state of chronic sulfide-mediated metabolic stress. Evidence from a clinical study in non-DS subjects reported that Hashimoto's thyroiditis patients show reduced microbial capacity for dissimilatory sulfate reduction-mediated H_2S production, with lower serum H_2S correlating with higher thyroglobulin antibody titers; H_2S supplementation ameliorated thyroid autoimmunity in an experimental mouse model [48]. In DS, the constitutive interferon hyperactivation [38, 39] creates an inflammatory backdrop, further evidenced by elevated IL-16 and IFN-γ levels associated with increased SOD1 expression [47], in which reduced microbial H_2S production could plausibly amplify thyroid autoimmune vulnerability [48]. This hypothesis remains untested in DS models and warrants targeted experimental validation. Enhancing H_2S catabolism via gut microbiota modulation, such as probiotics favoring low-sulfur bacteria or sulfur-restricted diets, presents a targeted therapy to alleviate DS bioenergetic and neurological deficits.

In the comparison of DS children with versus without immunological disease comorbidities, the simultaneous downregulation of Glycolysis/Gluconeogenesis, Pyruvate metabolism, and Oxidative phosphorylation in the comorbid group, in both age groups, represents a potentially fundamental impairment of microbial central energy metabolism. Butanoate (butyrate) metabolism was also among the most prominently downregulated pathways. Consistent with this, Cai et al. [11] reported significantly reduced *Anaerostipes* and *Parasutterella*, key butyrate-producing taxa, in DS adults, pointing to a diminished fermentative capacity in DS. The concurrent downregulation of these interconnected energy pathways may substantially reduce SCFA production, and butyrate in particular, which is critical for colonocyte energy supply, gut barrier integrity, and Foxp3+ Treg cell differentiation [49]. Butyrate acts as an Histone Deacetylase (HDAC) inhibitor that promotes Foxp3+

Treg differentiation [49]; in murine colonocytes, butyrate-activated PPAR-γ signalling sustains epithelial hypoxia and suppresses *Enterobacteriaceae* expansion [50], so impairment of this axis may perpetuate a self-reinforcing cycle of dysbiosis and immune activation. Because DS children already exhibit reduced and functionally impaired Treg populations [51], a microbiota-driven butyrate deficiency in the comorbid subgroup may synergise with these intrinsic Treg deficits to amplify autoimmune and inflammatory comorbidity risk [9, 11, 51]. Unlike the abundance-based findings of Cai et al., our metaproteomic data identify other taxa actively expressing butanoate-metabolism enzymes: Lachnospiraceae and Prevotellaceae (mainly *Coprococcus* and *Segatella*, formerly *Prevotella*) in the younger group, and Lachnospiraceae (*Blautia*) with Oscillospiraceae (*Oscillibacter*) in the older group. This shift from presence to expressed function likely accounts for the different taxa recovered. Beyond immune regulation, the same SCFA depletion may extend to the neurobehavioral phenotype of DS: dysbiosis and altered GM metabolites can affect brain development and behavior, and SCFAs such as butyrate, acetate, produced through the fermentation of dietary fibers, have been identified as important mediators in gut-brain axis communication, potentially influencing brain function via systemic circulation and transporter-dependent mechanisms at the BBB [52]. Intriguingly, one of the butanoate-metabolism-associated taxa in our younger cohort, *Segatella*, sits at this immune-behavioral interface, having been implicated in both SCFA metabolism and DS-associated behaviors. This gut-brain dimension is particularly relevant in DS, where behavioral and neuropsychiatric comorbidities are frequent, clinically heterogeneous, and developmentally dynamic. Behavioral presentations in neurodevelopmental disorders reflect complex interactions among genetic, cognitive, and behavioral domains, illustrating the multifactorial nature of these conditions [53]. In DS, behavioral challenges are common, with 20-40% of children experiencing recognized difficulties [54]. Throughout their lifespan, approximately half of individuals with DS encounter significant mental health issues, including anxiety, obsessive-compulsive symptoms, oppositional behaviors, depression, and tic disorders. The behavioral profile varies across development: childhood presentations often feature externalizing symptoms like aggression and attention problems, while internalizing symptoms such as depression and social withdrawal emerge later [55]. A notable subset also exhibits autism spectrum disorder features [56, 57]. The stratification of our cohort based on the presence or absence of these comorbidities is therefore crucial, as these conditions may represent distinct phenotypic subgroups with potentially different underlying biological mechanisms. Emerging evidence links gastrointestinal function to behavioral outcomes in DS. Maladaptive behaviors correlated with altered gut bacterial profiles in adults [10], and another work extended this connection to diagnosed GI disorders in younger individuals with DS [58]. Experimental studies demonstrate that fecal microbiota from DS

individuals or *S. copri* administration in mice induces DS-associated behaviors, including depressive-like symptoms and motor impairments [11]. These findings suggest the enriched *S. copri* in DS may contribute to behavioral manifestations through microbiome-mediated mechanisms. This closes a loop with our own data: *Segatella* emerged among the butanoate-metabolism-associated taxa in our younger age group in presence of immunological comorbidities, yet the same taxon acts as a behavior-worsening factor in Cai's model, pointing to a context-dependent role, in which the net effect of *Segatella* likely hinges on strain, co-occurring taxa, and host background rather than on its mere presence

In our study, in presence of behavioral features the convergent down-regulation across the sixteen target KEGG pathways, in both age-dependent comparisons, pointed out to, again, a coordinated loss of microbial functional capacity spanning amino-acid, carbohydrate, nucleotide and glycan-directed modules. Comorbidity in DS is accompanied by a broadly hypofunctional, SCFA-poor microbial metabolic state linked to amino-acid metabolism. Tryptophan and tyrosine metabolism, arginine and proline metabolism, branched-chain amino-acid (valine, leucine and isoleucine) degradation, and the upstream 2-oxocarboxylic acid metabolism were all decreased, a coherent contraction of the microbial supply of neurotransmitter precursors along the GM-GBA, in which tryptophan metabolism and SCFAs are principal routes of gut-to-brain communication [52]. These pathways are anchored in the DS literature, where tyrosine metabolism was among the pathways altered in the DS faecal metabolome [11]. As already described, critically, this links back to the butanoate signal in DS specifically: the butyrate-related genus *Blautia* has been associated with cognitive function in DS children [13], altered gut microbiota correlates with cognitive impairment in DS children [12], DS-specific microbial signatures correlate with behavioral (ABC) scores [10], and microbiome alterations distinguish cognitively stable from impaired adults with DS [9]. Together these suggest that the behavioral and immunological comparisons in our cohort may share a common butyrate- and amino-acid-related substrate. A second group of pathways points to the biosynthetic and energetic backbone that sustains fermentation. Pyrimidine metabolism and fructose and mannose metabolism were by far the most heavily populated pathways in both comparisons (63 and 42 PGs, respectively), indicating that the functional contraction extended to nucleotide biosynthesis and salvage and to central sugar catabolism. Because these routes feed the carbon and energy flux from which colonic SCFAs, and butanoate in particular, are ultimately generated, their reduction is mechanistically consistent with, and provides an upstream explanation for, the butanoate signal already noted in this cohort: a down-regulated fermentation network is expected to translate into diminished butyrate-generating capacity. A third module concerns host- and dietary-glycan foraging. Other glycan degradation,

glycosaminoglycan degradation, glycosphingolipid biosynthesis (globo/isoglobo and ganglio series) and various types of N-glycan biosynthesis were also reduced. Mucin- and host-glycan-directed catabolism is a broadly distributed capacity of the GM and a key determinant of niche competition at the mucosal interface [59]; its contraction is coherent with the same hypofunctional state and could plausibly bear on epithelial-barrier interactions in DS. Finally, the reduced fermentation output links this metabolic picture to the immunological comparison: SCFAs such as butyrate and propionate are established regulators of colonic regulatory-T-cell homeostasis and of the Treg/Th17 balance [60, 61] placing an SCFA-poor microbiota at the intersection of gut immunometabolism and comorbidity [62]. Mapping the down-regulated PGs onto taxonomy shows that metaproteomics evidenced that the functional contraction is carried by a limited, recurring set of organisms rather than distributed evenly. At genus level the broadest carriers were Bacteroides (spanning 12 of the 16 pathways) and Phocaeicola (10 pathways), consistent with the versatile metabolic repertoire of Bacteroidota. The functionally decisive recurrence, however, was among the butyrate-associated Bacillota: *Faecalibacterium*, *Blautia* and *Ruminococcus bromii* reappeared across the amino-acid and fermentation modules. *Faecalibacterium prausnitzii* alone contributed reduced PGs to seven pathways, and all eight of its amino-acid-pathway PGs were down-regulated (mean $\log_{10}$FC ≈ -0.37), while *Blautia* recurred across 2-oxocarboxylic acid, tyrosine and BCAA metabolism. Because *F. prausnitzii* and *Blautia* are among the principal butyrate producers of the colon, their concurrent, multi-pathway down-regulation supplies the taxonomic bridge to the DS-specific literature: the butyrate-related genus *Blautia* has been associated with cognitive function in DS children [13], altered gut microbiota correlates with cognitive impairment in DS children [12], DS-specific microbial signatures track behavioural (ABC) scores [10], microbiome alterations distinguish cognitively stable from impaired adults with DS [9] and comparable shifts are detectable even in twins discordant for DS [28]. The recurrence of the same butyrogenic taxa across the reduced amino-acid and fermentation pathways therefore suggests that the behavioural and immunological comparisons in this cohort share a common butyrate- and amino-acid-related substrate.

A substantial fraction of the human PGs recovered in feces mapped to collagen biosynthesis, collagen trimerization and degradation, ECM proteoglycans, fibronectin matrix formation, and integrin and syndecan interactions, and differential analysis further highlighted the MET signaling pathway. This ECM-centered signature is consistent with the dosage-sensitive dysregulation of the extracellular matrix in T21: the type VI collagen genes COL6A1 and COL6A2 map to chromosome 21q22.3 and are overexpressed in DS, with altered ECM architecture and increased collagen VI deposition documented in DS-derived tissues and fibroblasts [63]. At the systemic level, previous proteomic

work has reported that ECM-related proteins are broadly depleted in the plasma proteome of T21 individuals, suggesting impaired regulation of organ development and tissue homeostasis [64]. ECM remodeling has likewise emerged as a significantly altered process across independent DS models, including the liver transcriptome of a T21 mouse model and trisomic iPSC-derived endothelial and mesodermal cells, where dysregulation of collagens, fibronectin, and matrix metalloproteinases was observed [65–67]. Together with the enrichment of receptor-tyrosine-kinase signaling, this points to a coordinated program of matrix turnover, adhesion, and cell motility that is recapitulated in the fecal host proteome, also in relation to patient comorbidities. Beyond the ECM, the fecal proteome captured additional programs known to be driven by chromosome 21 gene dosage. Most directly, we identified liver-type 6-phosphofructokinase (PFKL), a chromosome 21q22.3 gene whose dosage-driven over-activity is an hallmark of T21 [68, 69], together with a cluster of glycolytic, gluconeogenic, and mitochondrial-carrier proteins and the antioxidant peroxiredoxin-2, consistent with the altered energy metabolism and chronic oxidative stress now regarded as core, cross-tissue features of the syndrome [70, 71]. In parallel, the interferon-stimulated protein IFITM1, alongside immunoglobulin chains and immune-effector proteins, mirrors the constitutive interferon activation attributed to the four interferon receptors encoded on chromosome 21 [37], a signal of particular relevance to the immunological comorbidities used for stratification.

In conclusion, the dominant pattern in this study was a broad, coordinated down-regulation of microbial protein expression across energy-yielding, fermentative and amino-acid pathways, rather than isolated changes in single functions. Because metaproteomics quantifies the enzymes the GM actually expresses rather than its inferred genetic potential, this is best read as functional reprogramming of the microbial community associated with each clinical phenotype. The signal was most marked in the immunological subgroup and centered on butanoate and its supporting energy and fermentation network, a direction consistent with the depletion of Bacillota proteins in carbohydrate, energy and amino-acid metabolism and SCFA production reported in a large gut-metaproteomic cohort [72], supporting a model in which comorbidity in DS is accompanied by a hypofunctional, SCFA-poor microbial metabolic state. To our knowledge, this is one of the first protein-level functional read-outs of how the microbiome tracks comorbidity in this population (**Figure 7**).

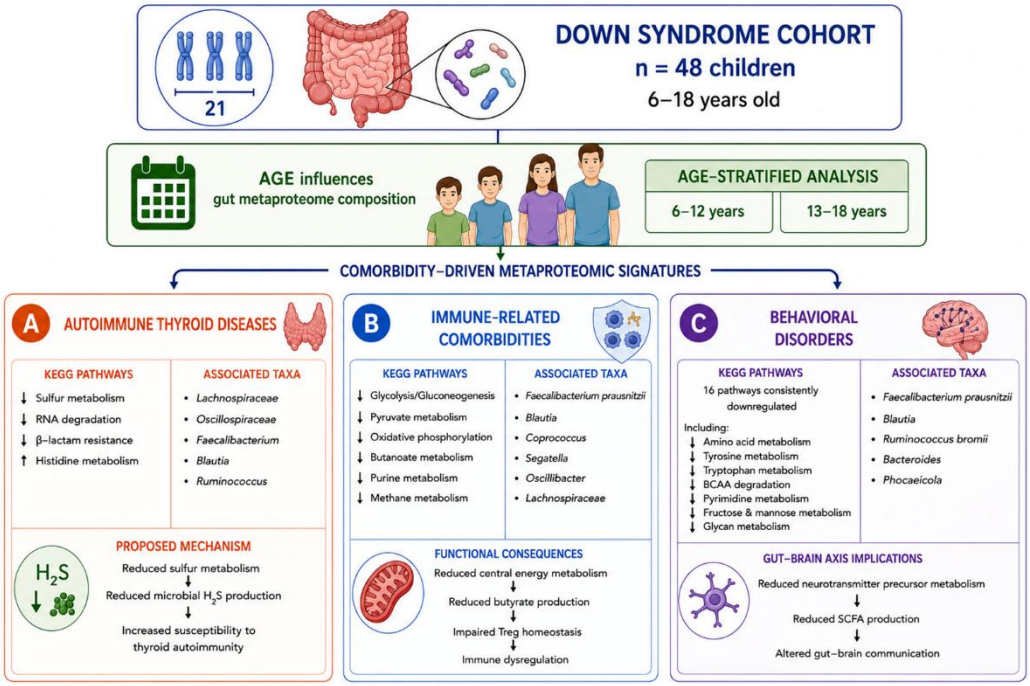


Figure 7. Functional contraction of the gut metaproteome in children with Down syndrome and comorbidities. Study overview (n = 48, 6–18 years, stratified into 6–12 and 13–18 years) and comorbidity-specific metaproteomic signatures for autoimmune thyroid diseases (A), immune-related comorbidities (B), and behavioral disorders (C), showing differentially represented KEGG pathways, associated taxa, and proposed functional consequences (↓ depleted, ↑ enriched).

Taken together, these findings indicate that the genetics of T21 is necessary but may be not sufficient to explain the clinical picture: in an accessible peripheral sample, the fecal host proteome recapitulates several dosage-driven programs of T21, matrix remodeling, energy metabolism and interferon-skewed immunity, that track with the thyroid, immunological and behavioral comorbidities used for stratification. The GM represents a plausible, though still speculative, integrative layer, and defining its contribution will require dedicated functional and longitudinal studies. Our results align with a recent multi-omic deconvolution of Down syndrome showing that the biological consequences of T21 cannot be fully understood without accounting for co-occurring conditions [64]; we extend this perspective to the GM, supporting comorbidity-stratified fecal biomarkers as a further step toward precision medicine in DS.

5 Statements & Declarations

5.1 Funding

This study was funded by Lazio Innova (Regione Lazio), project “Human Genome Project-Trisomy 21 (HGP-T21)”. The Italian Ministry of Health provided “Current Research funds” to support this work.

5.2 Competing Interests

Pirona I., Macari G., and Gardini S. were employed by GenomeUp. All other authors declare no potential conflict of interest.

5.3 Author Contributions

BDP, GS, VD, and LP: conceptualization and funding acquisition. GM, AN, GS, VD, AV, and LP: supervision. VM and LP: design of the study, writing, original draft preparation, and editing. VM, IP, FR, MC, LMS, VP, EA, and VD: investigation. VM, IP, and CM: visualization. All authors contributed to the article and approved the submitted version.

5.4 Data Availability

The MS data presented in the study are available on the MASSIVE public repository (https://massive.ucsd.edu/ProteoSAFe/static/massive.jsp) with the identifier code MSV000095483. The dataset is currently private and will be made publicly available as soon as the article is accepted. A dedicated reviewer account has been created for this dataset, which allows the files to be accessed and reviewed while the submission remains private. The credentials, to be used at https://massive.ucsd.edu/ProteoSAFe/static/massive.jsp, are:

Username: MSV000095483_reviewer

Password: Down_July2024

5.5 Ethics approval and Consent to participate

The study protocol was conducted in accordance with the Principles of Good Clinical Practice and the Declaration of Helsinki, and approved by the OPBG Ethical Committee (protocol code HGP-T21/2632_OPBG_2021). Written informed consent was obtained from parents or legal representatives of children participating in the study. We are profoundly grateful to the children and their families whose willingness to participate made this research achievable.

6 References

1. Moore SW (2008) Down syndrome and the enteric nervous system. Pediatr Surg Int 24:873–883. https://doi.org/10.1007/s00383-008-2188-7

2. Stoll C, Dott B, Alembik Y, Roth M-P (2015) Associated congenital anomalies among cases with Down syndrome. Eur J Med Genet 58:674–680. https://doi.org/10.1016/j.ejmg.2015.11.003

3. Ravel A, Mircher C, Rebillat A-S, et al (2020) Feeding problems and gastrointestinal diseases in Down syndrome. Archives de Pédiatrie 27:53–60. https://doi.org/10.1016/j.arcped.2019.11.008

4. Antonarakis SE, Skotko BG, Rafii MS, et al (2020) Down syndrome. Nat Rev Dis Primers 6:9. https://doi.org/10.1038/s41572-019-0143-7

5. Bull MJ (2020) Down Syndrome. N Engl J Med 382:2344–2352. https://doi.org/10.1056/NEJMra1706537

6. Dierssen M (2012) Down syndrome: the brain in trisomic mode. Nat Rev Neurosci 13:844–858. https://doi.org/10.1038/nrn3314

7. Borrego-Ruiz A, Borrego JJ (2024) Neurodevelopmental Disorders Associated with Gut Microbiome Dysbiosis in Children. Children 11:796. https://doi.org/10.3390/children11070796

8. González-Parra JA, Barrera-Conde M, Kossatz E, et al (2025) Microbiota and social behavior alterations in a mouse model of down syndrome: Modulation by a synbiotic treatment. Prog Neuropsychopharmacol Biol Psychiatry 136:111200. https://doi.org/10.1016/j.pnpbp.2024.111200

9. Rosas HD, Morgan XC, Tao Y, et al (2025) Gut dysbiosis in Down syndrome: A potentially unexplored culprit for early Alzheimer's disease. Alzheimers Dement 21:e70330. https://doi.org/10.1002/alz.70330

10. Biagi E, Candela M, Centanni M, et al (2014) Gut Microbiome in Down Syndrome. PLoS ONE 9:e112023. https://doi.org/10.1371/journal.pone.0112023

11. Cai S, Lin J, Li Z, et al (2023) Alterations in intestinal microbiota and metabolites in individuals with Down syndrome and their correlation with inflammation and behavior disorders in mice. Front Microbiol 14:1016872. https://doi.org/10.3389/fmicb.2023.1016872

12. Ren S, Wang X, Qin J, et al (2022) Altered gut microbiota correlates with cognitive impairment in Chinese children with Down's syndrome. Eur Child Adolesc Psychiatry 31:189–202. https://doi.org/10.1007/s00787-021-01799-2

13. Hou X, Wu N, Ren S, et al (2023) Profiling Blautia at high taxonomic resolution reveals correlations with cognitive dysfunction in Chinese children with Down syndrome. Front Cell Infect Microbiol 13:1109889. https://doi.org/10.3389/fcimb.2023.1109889

14. Lynch SV, Pedersen O (2016) The Human Intestinal Microbiome in Health and Disease. N Engl J Med 375:2369–2379. https://doi.org/10.1056/NEJMra1600266

15. Putignani L, Del Chierico F, Petrucca A, et al (2014) The human gut microbiota: a dynamic interplay with the host from birth to senescence settled during childhood. Pediatr Res 76:2–10. https://doi.org/10.1038/pr.2014.49

16. Levi Mortera S, Marzano V, Rapisarda F, et al (2024) Metaproteomics reveals diet-induced changes in gut microbiome function according to Crohn's disease location. Microbiome 12:217. https://doi.org/10.1186/s40168-024-01927-5

17. Marzano V, Levi Mortera S, Marangelo C, et al (2023) The metaproteome of the gut microbiota in pediatric patients affected by COVID-19. Front Cell Infect Microbiol 13:1327889. https://doi.org/10.3389/fcimb.2023.1327889

18. Distler U, Kuharev J, Navarro P, Tenzer S (2016) Label-free quantification in ion mobility-enhanced data-independent acquisition proteomics. Nat Protoc 11:795–812. https://doi.org/10.1038/nprot.2016.042

19. Cheng K, Ning Z, Li L, et al (2023) MetaLab-MAG: A Metaproteomic Data Analysis Platform for Genome-Level Characterization of Microbiomes from the Metagenome-Assembled Genomes Database. J Proteome Res 22:387–398. https://doi.org/10.1021/acs.jproteome.2c00554

20. Almeida A, Nayfach S, Boland M, et al (2021) A unified catalog of 204,938 reference genomes from the human gut microbiome. Nat Biotechnol 39:105–114. https://doi.org/10.1038/s41587-020-0603-3

21. Gurbich TA, Almeida A, Beracochea M, et al (2023) MGnify Genomes: A Resource for Biome-specific Microbial Genome Catalogues. Journal of Molecular Biology 435:168016. https://doi.org/10.1016/j.jmb.2023.168016

22. Kanehisa M, Furumichi M, Sato Y, et al (2025) KEGG: biological systems database as a model of the real world. Nucleic Acids Res 53:D672–D677. https://doi.org/10.1093/nar/gkae909

23. Kanehisa M, Goto S (2000) KEGG: Kyoto Encyclopedia of Genes and Genomes. Nucleic Acids Res 28:27–30. https://doi.org/10.1093/nar/28.1.27

24. Thomas PD, Ebert D, Muruganujan A, et al (2022) PANTHER: Making genome-scale phylogenetics accessible to all. Protein Science 31:8–22. https://doi.org/10.1002/pro.4218

25. Fonseka P, Pathan M, Chitti SV, et al (2021) FunRich enables enrichment analysis of OMICs datasets. Journal of Molecular Biology 433:166747. https://doi.org/10.1016/j.jmb.2020.166747

26. Griss J, Viteri G, Sidiropoulos K, et al (2020) ReactomeGSA - Efficient Multi-Omics Comparative Pathway Analysis. Molecular & Cellular Proteomics 19:2115–2125. https://doi.org/10.1074/mcp.TIR120.002155

27. Alkuwaiti SH, Skrabulyte-Barbulescu J, Yassin LK, et al (2025) Harnessing the microbiota-gut–brain axis to prevent and treat pediatric neurodevelopmental disorders: translational insights and strategies. J Transl Med 23:1286. https://doi.org/10.1186/s12967-025-07279-4

28. Maillard P-Y, Tokajian S, Vilaire-Meunier M, et al (2025) Gut Microbial Similarity Analysis in Mono and Dizygotic Twins Discordant for Down Syndrome. OBM Genet 09:1–22. https://doi.org/10.21926/obm.genet.2503300

29. Liu Y, Hu D, Dai C, et al (2021) Characteristics of Intestinal Microbiota and Mother's Reproductive Tract Flora in Children With Down Syndrome

30. Stamboulian M, Canderan J, Ye Y (2022) Metaproteomics as a tool for studying the protein landscape of human-gut bacterial species. PLoS Comput Biol 18:e1009397. https://doi.org/10.1371/journal.pcbi.1009397

31. Marzano V, Levi Mortera S, Putignani L (2025) Insights on Wet and Dry Workflows for Human Gut Metaproteomics. Proteomics 25:230–252. https://doi.org/10.1002/pmic.202400242

32. Buczyńska A, Sidorkiewicz I, Trochimiuk A, et al (2021) Novel Approaches to an Integrated Route for Trisomy 21 Evaluation. Biomolecules 11:1328. https://doi.org/10.3390/biom11091328

33. Marzano V, Levi Mortera S, Vernocchi P, et al (2023) Williams-Beuren syndrome shapes the gut microbiota metaproteome. Sci Rep 13:18963. https://doi.org/10.1038/s41598-023-46052-9

34. Metwalley KA, Farghaly HS (2022) Endocrinal dysfunction in children with Down syndrome. Ann Pediatr Endocrinol Metab 27:15–21. https://doi.org/10.6065/apem.2142236.118

35. Hom B, Boyd NK, Vogel BN, et al (2024) Down Syndrome and Autoimmune Disease. Clinic Rev Allerg Immunol 66:261–273. https://doi.org/10.1007/s12016-024-08996-2

36. Ferrari M, Stagi S (2021) Autoimmunity and Genetic Syndromes: A Focus on Down Syndrome. Genes 12:268. https://doi.org/10.3390/genes12020268

37. Sullivan KD, Lewis HC, Hill AA, et al (2016) Trisomy 21 consistently activates the interferon response. eLife 5:e16220. https://doi.org/10.7554/eLife.16220

38. Chung H, Green PHR, Wang TC, Kong X-F (2021) Interferon-Driven Immune Dysregulation in Down Syndrome: A Review of the Evidence. J Inflamm Res 14:5187–5200. https://doi.org/10.2147/JIR.S280953

39. Galbraith MD, Rachubinski AL, Smith KP, et al (2023) Multidimensional definition of the interferonopathy of Down syndrome and its response to JAK inhibition. Science Advances 9:eadg6218. https://doi.org/10.1126/sciadv.adg6218

40. Waugh KA, Minter R, Baxter J, et al (2023) Triplication of the interferon receptor locus contributes to hallmarks of Down syndrome in a mouse model. Nat Genet 55:1034–1047. https://doi.org/10.1038/s41588-023-01399-7

41. Malle L, Patel RS, Martin-Fernandez M, et al (2023) Autoimmunity in Down's syndrome via cytokines, CD4 T cells and CD11c+ B cells. Nature 615:305–314. https://doi.org/10.1038/s41586-023-05736-y

42. Wang G, Shi W, Liao S, Hao B (2026) Revisiting down syndrome through the lens of interferonopathy and innate immune dysregulation. Front Immunol 17:. https://doi.org/10.3389/fimmu.2026.1836558

900 43. Gans M, Wyke M, Somay K, et al (2026) How I Treat: Immune dysregulation in Down
901 syndrome. Journal of Human Immunity 2:e20250161. https://doi.org/10.70962/jhi.20250161

902 44. Kanemaru E, Ichinose F (2025) Essential role of sulfide oxidation in brain health and
903 neurological disorders. Pharmacology & Therapeutics 266:108787.
904 https://doi.org/10.1016/j.pharmthera.2024.108787

905 45. Cirino G, Szabo C, Papapetropoulos A (2023) Physiological roles of hydrogen sulfide in
906 mammalian cells, tissues, and organs. Physiol Rev 103:31–276.
907 https://doi.org/10.1152/physrev.00028.2021

908 46. Buret AG, Allain T, Motta J-P, Wallace JL (2022) Effects of Hydrogen Sulfide on the
909 Microbiome: From Toxicity to Therapy. Antioxidants & Redox Signaling 36:211–219.
910 https://doi.org/10.1089/ars.2021.0004

911 47. Mouli K, Liopo AV, Wang H, et al (2026) Transcriptomic and proteomic evidence for
912 noncanonical hydrogen sulfide metabolism and immune dysregulation in Down Syndrome. Sci
913 Rep. https://doi.org/10.1038/s41598-026-45627-6

914 48. Zhang S, Zhao X, Wang X, et al (2024) Gut Microecology May Be Involved in the
915 Pathogenesis of Hashimoto Thyroiditis by Reducing Production of Hydrogen Sulfide. J Clin
916 Endocrinol Metab 109:792–801. https://doi.org/10.1210/clinem/dgad588

917 49. Furusawa Y, Obata Y, Fukuda S, et al (2013) Commensal microbe-derived butyrate induces
918 the differentiation of colonic regulatory T cells. Nature 504:446–450.
919 https://doi.org/10.1038/nature12721

920 50. Byndloss MX, Olsan EE, Rivera-Chávez F, et al (2017) Microbiota-activated PPAR-γ
921 signaling inhibits dysbiotic Enterobacteriaceae expansion. Science 357:570–575.
922 https://doi.org/10.1126/science.aam9949

923 51. Huggard D, Doherty DG, Molloy EJ (2020) Immune Dysregulation in Children With Down
924 Syndrome. Front Pediatr 8:73. https://doi.org/10.3389/fped.2020.00073

925 52. Silva YP, Bernardi A, Frozza RL (2020) The Role of Short-Chain Fatty Acids From Gut
926 Microbiota in Gut-Brain Communication. Front Endocrinol (Lausanne) 11:25.
927 https://doi.org/10.3389/fendo.2020.00025

928 53. Harris JC (2010) Advances in understanding behavioral phenotypes in neurogenetic
929 syndromes. American J of Med Genetics Pt C 154C:389–399.
930 https://doi.org/10.1002/ajmg.c.30276

931 54. Visootsak J, Sherman S (2007) Neuropsychiatric and behavioral aspects of trisomy 21. Curr
932 Psychiatry Rep 9:135–140. https://doi.org/10.1007/s11920-007-0083-x

933 55. McGuire D, Chicoine B (2021) Mental Wellness in Adults with Down Syndrome, A Guide to
934 Emotional and Behavioral Strengths and Challenges, Second Edition. Woodbine House
935 Publishing

936 56. Capone GT, Grados MA, Kaufmann WE, et al (2005) Down syndrome and comorbid autism-
937 spectrum disorder: Characterization using the aberrant behavior checklist. American J of Med
938 Genetics Pt A 134A:373–380. https://doi.org/10.1002/ajmg.a.30622

57. Dykens EM (2007) Psychiatric and behavioral disorders in persons with Down syndrome. Ment Retard Dev Disabil Res Rev 13:272–278. https://doi.org/10.1002/mrdd.20159

58. Schworer EK, Ahmed A, Hogenkamp L, et al (2022) Associations among co-occurring medical conditions and cognition, language, and behavior in Down syndrome. Research in Developmental Disabilities 126:104236. https://doi.org/10.1016/j.ridd.2022.104236

59. Ravcheev DA, Thiele I (2017) Comparative Genomic Analysis of the Human Gut Microbiome Reveals a Broad Distribution of Metabolic Pathways for the Degradation of Host-Synthetized Mucin Glycans and Utilization of Mucin-Derived Monosaccharides. Front Genet 8:111. https://doi.org/10.3389/fgene.2017.00111

60. Smith PM, Howitt MR, Panikov N, et al (2013) The Microbial Metabolites, Short-Chain Fatty Acids, Regulate Colonic T_{reg} Cell Homeostasis. Science 341:569–573. https://doi.org/10.1126/science.1241165

61. Su X, Yin X, Liu Y, et al (2020) Gut Dysbiosis Contributes to the Imbalance of Treg and Th17 Cells in Graves' Disease Patients by Propionic Acid. The Journal of Clinical Endocrinology & Metabolism 105:3526–3547. https://doi.org/10.1210/clinem/dgaa511

62. Belizário JE, Faintuch J, Garay-Malpartida M (2018) Gut Microbiome Dysbiosis and Immunometabolism: New Frontiers for Treatment of Metabolic Diseases. Mediators of Inflammation 2018:1–12. https://doi.org/10.1155/2018/2037838

63. Karousou E, Stachtea X, Moretto P, et al (2013) New insights into the pathobiology of Down syndrome--hyaluronan synthase-2 overexpression is regulated by collagen VI α2 chain. FEBS J 280:2418–2430. https://doi.org/10.1111/febs.12220

64. Donovan MG, Chillamcherla S, Enriquez Estrada BA, et al (2026) Systematic multi-omic deconvolution of the clinical heterogeneity of Down syndrome. Nat Commun. https://doi.org/10.1038/s41467-026-72946-z

65. Dunn LN, Niemeyer BF, Eduthan NP, et al (2026) Altered hepatic metabolism in Down syndrome. Cell Reports 45:116835. https://doi.org/10.1016/j.celrep.2025.116835

66. Galat Y, Perepitchka M, Elcheva I, et al (2020) iPSC-derived progenitor stromal cells provide new insights into aberrant musculoskeletal development and resistance to cancer in down syndrome. Sci Rep 10:13252. https://doi.org/10.1038/s41598-020-69418-9

67. Perepitchka M, Galat Y, Beletsky IP, et al (2020) Down syndrome iPSC model: endothelial perspective on tumor development. Oncotarget 11:3387–3404. https://doi.org/10.18632/oncotarget.27712

68. Elson A, Levanon D, Weiss Y, Groner Y (1994) Overexpression of liver-type phosphofructokinase (PFKL) in transgenic-PFKL mice: implication for gene dosage in trisomy 21. Biochem J 299 (Pt 2):409–415. https://doi.org/10.1042/bj2990409

69. Vora S, Francke U (1981) Assignment of the human gene for liver-type 6-phosphofructokinase isozyme (PFKL) to chromosome 21 by using somatic cell hybrids and monoclonal anti-L antibody. Proc Natl Acad Sci U S A 78:3738–3742. https://doi.org/10.1073/pnas.78.6.3738

70. Dierssen M, Fructuoso M, Martínez de Lagrán M, et al (2020) Down Syndrome Is a Metabolic Disease: Altered Insulin Signaling Mediates Peripheral and Brain Dysfunctions. Front Neurosci 14:670. https://doi.org/10.3389/fnins.2020.00670

71. Izzo A, Mollo N, Nitti M, et al (2018) Mitochondrial dysfunction in down syndrome: molecular mechanisms and therapeutic targets. Mol Med 24:2. https://doi.org/10.1186/s10020-018-0004-y

72. Liang S, Sun Y, Miao Z, et al (2026) Large-scale metaproteomics of human gut microbiota reveals microbial functions in metabolic diseases and aging. Cell Metabolism 38:995-1011.e6. https://doi.org/10.1016/j.cmet.2026.02.012

Supplementary Files

This is a list of supplementary files associated with this preprint. Click to download.

- SupplementaryFile231072026.xlsx
- SupplementaryFile731072026.xlsx
- SupplementaryFile431072026.xlsx
- SupplementaryFile631072026.xlsx
- SupplementaryFile131072026.xlsx
- SupplementaryFile531072026.xlsx
- SupplementaryFig15.docx
- SupplementaryFile331072026.xlsx